

1 Secondary Organic Aerosols from Anthropogenic Volatile Organic Compounds Contribute 2 Substantially to Air Pollution Mortality

3

4 Benjamin A. Nault^{1,2,*}, Duseong S. Jo^{1,2}, Brian C. McDonald^{2,3}, Pedro Campuzano-Jost^{1,2}, Douglas A.
5 Day^{1,2}, Weiwei Hu^{1,2,**}, Jason C. Schroder^{1,2,***}, James Allan^{4,5}, Donald R. Blake⁶, Manjula R.
6 Canagaratna⁷, Hugh Coe⁵, Matthew M. Coggon^{2,3}, Peter F. DeCarlo⁸, Glenn S. Diskin⁹, Rachel
7 Dunmore¹⁰, Frank Flocke¹¹, Alan Fried¹², Jessica B. Gilman³, Georgios Gkatzelis^{2,3,****}, Jacqui F.
8 Hamilton¹⁰, Thomas F. Hanisco¹³, Patrick L. Hayes¹⁴, Daven K. Henze¹⁵, Alma Hodzic^{11,16}, James
9 Hopkins^{10,17}, Min Hu¹⁸, L. Gregory Huey¹⁹, B. Thomas Jobson²⁰, William C. Kuster^{3,*****}, Alastair
10 Lewis^{10,17}, Meng Li^{2,3}, Jin Liao^{13,21}, M. Omar Nawaz¹⁵, Ilana B. Pollack²², Jeffrey Peischl^{2,3}, Bernhard
11 Rappenglück²³, Claire E. Reeves²⁴, Dirk Richter¹², James M. Roberts³, Thomas B. Ryerson^{3,*****}, Min
12 Shao²⁵, Jacob M. Sommers^{14,26}, James Walega¹², Carsten Warneke^{2,3}, Petter Weibring¹², Glenn M.
13 Wolfe^{13,27}, Dominique E. Young^{5,*****}, Bin Yuan²⁵, Qiang Zhang²⁸, Joost A. de Gouw^{1,2}, and Jose L.
14 Jimenez^{1,2,+}

15

16 1. Department of Chemistry, University of Colorado, Boulder, Boulder, CO, USA

17 2. Cooperative Institute for Research in Environmental Sciences, Boulder, Colorado, USA

18 3. Chemical Sciences Division, NOAA Earth System Research Laboratory, Boulder, CO

19 4. National Centre for Atmospheric Sciences, School of Earth and Environmental Sciences, University of Manchester, Manchester, UK

20 5. Centre of Atmospheric Science, School of Earth and Environmental Sciences, University of Manchester, Manchester, UK

21 6. Department of Chemistry, University of California, Irvine, Irvine, CA, USA

22 7. Center for Aerosol and Cloud Chemistry, Aerodyne Research Inc., Billerica, MA, USA

23 8. Department of Environmental Health Engineering, Johns Hopkins University, Baltimore, MD, USA

24 9. NASA Langley Research Center, Hampton, Virginia, USA

25 10. Wolfson Atmospheric Chemistry Laboratories, Department of Chemistry, University of York, York, UK

26 11. Atmospheric Chemistry Observations and Modeling Laboratory, National Center for Atmospheric Research, Boulder, CO, USA

27 12. Institute of Arctic and Alpine Research, University of Colorado, Boulder, CO, USA

28 13. Atmospheric Chemistry and Dynamic Laboratory, NASA Goddard Space Flight Center, Greenbelt, MD, USA

29 14. Department of Chemistry, Université de Montréal, Montréal, QC, Canada

30 15. Department of Mechanical Engineering, University of Colorado, Boulder, CO, USA

31 16. Laboratoires d'Aréologie, Université de Toulouse, CNRS, UPS, Toulouse, France

32 17. National Centre for Atmospheric Sciences, Department of Chemistry, University of York, York, UK

33 18. State Key Joint Laboratory of Environmental Simulation and Pollution Control, College of Environmental Sciences and Engineering, Peking

34 University, Beijing, China

35 19. School of Earth and Atmospheric Sciences, Georgia Institute of Technology, Atlanta, Georgia, USA

36 20. Laboratory for Atmospheric Research, Department of Civil and Environmental Engineering, Washington State University, Pullman, WA,

37 USA

38 21. Universities Space Research Association, GESTAR, Columbia, MD, USA

39 22. Department of Atmospheric Science, Colorado State University, Fort Collins, CO, USA

40 23. Department of Earth and Atmospheric Science, University of Houston, Houston, TX, USA

41 24. Centre for Ocean and Atmospheric Sciences, School of Environmental Sciences, University of East Anglia, Norwich, UK

42 25. Institute for Environmental and Climate Research, Jinan University, Guangzhou, China

43 26. Air Quality Research Division, Environment and Climate Change Canada, Toronto, Ontario, Canada

44 27. Joint Center for Earth Systems Technology, University of Maryland, Baltimore County, Baltimore, MD, USA

45 28. Ministry of Education Key Laboratory for Earth System Modeling, Department of Earth System Science, Tsinghua University, Beijing, China

46 *Now at Center for Aerosol and Cloud Chemistry, Aerodyne Research Inc., Billerica, MA, USA

47 **Now at State Key Laboratory at Organic Geochemistry, Guangzhou Institute of Geochemistry, Chinese Academy of Sciences, Guangzhou,

48 China

49 ***Now at Colorado Department of Public Health and Environment, Denver, CO, USA

50 ****Now at Forschungszentrum Juelich GmbH, Juelich, Germany

51 *****Has retired and worked on this manuscript as an unaffiliated co-author.

52 *****Now at Scientific Aviation, Boulder, CO, USA

53 *****Now at Air Quality Research Center, University of California, Davis, CA, USA

54

55

56 +Corresponding author: Jose L. Jimenez (jose.jimenez@colorado.edu)

57

58 **Abstract**

59 Anthropogenic secondary organic aerosol (ASOA), formed from anthropogenic emissions of
60 organic compounds, constitutes a substantial fraction of the mass of submicron aerosol in
61 populated areas around the world and contributes to poor air quality and premature mortality.
62 However, the precursor sources of ASOA are poorly understood, and there are large uncertainties
63 in the health benefits that might accrue from reducing anthropogenic organic emissions. We
64 show that the production of ASOA in 11 urban areas on three continents is strongly correlated
65 with the reactivity of specific anthropogenic volatile organic compounds. The differences in
66 ASOA production across different cities can be explained by differences in the emissions of
67 aromatics and intermediate- and semi-volatile organic compounds, indicating the importance of
68 controlling these ASOA precursors. With an improved modeling representation of ASOA driven
69 by the observations, we attribute 340,000 $PM_{2.5}$ premature deaths per year to ASOA, which is
70 over an order of magnitude higher than prior studies. A sensitivity case with a more recently
71 proposed model for attributing mortality to $PM_{2.5}$ (the Global Exposure Mortality Model) results
72 in up to 900,000 deaths. A limitation of this study is the extrapolation from cities with detailed
73 studies and regions where detailed emission inventories are available to other regions where
74 uncertainties in emissions are larger. In addition to further development of institutional air
75 quality management infrastructure, comprehensive air quality campaigns in the countries in
76 South and Central America, Africa, South Asia, and the Middle East are needed for further
77 progress in this area.

78 **1. Introduction**

79 Poor air quality is one of the leading causes of premature mortality worldwide (Cohen et
80 al., 2017; Landrigan et al., 2018). Roughly 95% of the world's population live in areas where
81 $PM_{2.5}$ (fine particulate matter with diameter smaller than 2.5 μm) exceeds the World Health
82 Organization's 10 $\mu g m^{-3}$ annual average guideline (Shaddick et al., 2018). This is especially true
83 for urban areas, where high population density is co-located with increased emissions of $PM_{2.5}$
84 and its gas-phase precursors from human activities. It is estimated that $PM_{2.5}$ leads to 3 to 4
85 million premature deaths per year, higher than the deaths associated with other air pollutants
86 (Cohen et al., 2017). More recent analysis using concentration-response relationships derived
87 from studies of populations exposure to high levels of ambient $PM_{2.5}$ suggest the global
88 premature death burden could be up to twice this value (Burnett et al., 2018).

89 The main method to estimate premature mortality with $PM_{2.5}$ is to use measured $PM_{2.5}$
90 from ground observations along with derived $PM_{2.5}$ from satellites to fill in missing ground-based
91 observations (van Donkelaar et al., 2015, 2016). To go from total $PM_{2.5}$ to species-dependent and
92 even sector-dependent associated premature mortality from $PM_{2.5}$, chemical transport models
93 (CTMs) are used to predict the fractional contribution of species and/or sector (e.g., Lelieveld et
94 al., 2015; van Donkelaar et al., 2015, 2016; Silva et al., 2016). However, though CTMs may get
95 total $PM_{2.5}$ or even total species, e.g., organic aerosol (OA), correct, the model may be getting the
96 values right for the wrong reason (e.g., de Gouw and Jimenez, 2009; Woody et al., 2016; Murphy
97 et al., 2017; Baker et al., 2018; Hodzic et al., 2020). This is especially important for OA in urban
98 areas, where models have a longstanding issue under predicting secondary OA (SOA) with some
99 instances of over predicting primary OA (POA) (de Gouw and Jimenez, 2009; Dzepina et al.,

100 2009; Hodzic et al., 2010b; Woody et al., 2016; Zhao et al., 2016a; Janssen et al., 2017; Jathar et
101 al., 2017). Further, this bias has even been observed for highly aged aerosols in remote regions
102 (Hodzic et al., 2020). As has been found in prior studies for urban areas (e.g., Zhang et al., 2007;
103 Kondo et al., 2008; Jimenez et al., 2009; DeCarlo et al., 2010; Hayes et al., 2013; Freney et al.,
104 2014; Hu et al., 2016; Nault et al., 2018; Schroder et al., 2018) and highlighted here (Fig. 1), a
105 substantial fraction of the observed submicron PM is OA, and a substantial fraction of the OA is
106 composed of SOA (approximately a factor of 2 to 3 higher than POA). Thus, to better understand
107 the sources and apportionment of $PM_{2.5}$ that contributes to premature mortality, CTMs must
108 improve their prediction of SOA versus POA, as the sources of SOA precursors and POA can be
109 different.

110 However, understanding the gas-phase precursors of photochemically-produced
111 anthropogenic SOA (ASOA, defined as the photochemically-produced SOA formed from the
112 photooxidation of anthropogenic volatile organic compounds (AVOC) (de Gouw et al., 2005;
113 DeCarlo et al., 2010)) quantitatively is challenging (Hallquist et al., 2009). Note, for the rest of
114 the paper, unless explicitly stated otherwise, ASOA refers to SOA produced from the
115 photooxidation of AVOCs, as there are potentially other relevant paths for the production of SOA
116 in urban environments (e.g., Petit et al., 2014; Kodros et al., 2018, 2020; Stavroulas et al., 2019).
117 Though the enhancement of ASOA is largest in large cities, these precursors and production of
118 ASOA should be important in any location impacted by anthropogenic emissions (e.g., Fig. 1).
119 ASOA comprises a wide range of condensable products generated by numerous chemical
120 reactions involving AVOC precursors (Hallquist et al., 2009; Hayes et al., 2015; Shrivastava et
121 al., 2017). The number of AVOC precursors, as well as the role of “non-traditional” AVOC

122 precursors, along with the condensable products and chemical reactions, compound to lead to
123 differences in the observed versus predicted ASOA for various urban environments (e.g., de
124 Gouw and Jimenez, 2009; Dzepina et al., 2009; Hodzic et al., 2010b; Woody et al., 2016; Janssen
125 et al., 2017; Jathar et al., 2017; McDonald et al., 2018). One solution to improve the prediction in
126 CTMs is to use a simplified model, where lumped ASOA precursors react, non-reversibly, at a
127 given rate constant, to produce ASOA (Hodzic and Jimenez, 2011; Hayes et al., 2015; Pai et al.,
128 2020). This simplified model has been found to reproduce the observed ASOA from some urban
129 areas (Hodzic and Jimenez, 2011; Hayes et al., 2015) but issues in other urban areas (Pai et al.,
130 2020). This may stem from the simplified model being parameterized to two urban areas (Hodzic
131 and Jimenez, 2011; Hayes et al., 2015). These inconsistencies impact the model predicted
132 fractional contribution of ASOA to total $PM_{2.5}$ and thus the ability to understand the source
133 attribution to $PM_{2.5}$ and premature deaths.

134 The main categories of gas-phase precursors that dominate ASOA have been the subject
135 of intensive research. The debate on what dominates can in turn impact the understanding of
136 what precursors to regulate to reduce ASOA, to improve air quality, and to reduce premature
137 mortality associated with ASOA. Transportation-related emissions (e.g., tailpipe, evaporation,
138 refueling) were assumed to be the major precursors of ASOA, which was supported by field
139 studies (Parrish et al., 2009; Gentner et al., 2012; Warneke et al., 2012; Pollack et al., 2013). Yet,
140 budget closure of observed ASOA mass concentrations could not be achieved with
141 transportation-related VOCs (Ensberg et al., 2014). The contribution of urban-emitted biogenic
142 precursors to SOA in urban areas is typically small. Biogenic SOA (BSOA) in urban areas
143 typically results from advection of regional background concentrations rather than processing of

144 locally emitted biogenic VOCs (e.g., Hodzic et al., 2009, 2010a; Hayes et al., 2013; Janssen et
145 al., 2017). BSOA is thought to dominate globally (Hallquist et al., 2009), but as shown in Fig. 1,
146 the contribution of BSOA (1% to 20%) to urban concentrations, while often substantial, is
147 typically smaller than that of ASOA (17% to 39%) (see Sect. S3.1).

148 Many of these prior studies generally investigated AVOC with high volatility, where
149 volatility here is defined as the saturation concentration, C^* , in $\mu\text{g m}^{-3}$ (de Gouw et al., 2005;
150 Volkamer et al., 2006; Dzepina et al., 2009; Freney et al., 2014; Woody et al., 2016). More recent
151 studies have identified lower volatility compounds in transportation-related emissions (e.g., Zhao
152 et al., 2014, 2016b; Lu et al., 2018). These compounds have been broadly identified as
153 intermediate-volatile organic compounds (IVOCs) and semi-volatile organic compounds
154 (SVOCs). IVOCs have a C^* generally of 10^3 to $10^6 \mu\text{g m}^{-3}$ while SVOCs have a C^* generally of
155 1 to $10^2 \mu\text{g m}^{-3}$. Due to their lower volatility and functional groups, these classes of compounds
156 generally form ASOA more efficiently than traditional, higher volatile AVOCs; however,
157 S/IVOCs have also been more difficult to measure (e.g., Zhao et al., 2014; Pagonis et al., 2017;
158 Deming et al., 2018). IVOCs generally have been the more difficult of the two classes to measure
159 and identify as these compounds cannot be collected onto filters to be sampled off-line (Lu et al.,
160 2018) and generally show up as unresolved complex mixture for in-situ measurements using
161 gas-chromatography (GC) (Zhao et al., 2014). SVOCs, on the other hand, can be more readily
162 collected onto filters and sampled off-line due to their lower volatility (Lu et al., 2018). Another
163 potential issue has been an under-estimation of the S/IVOC aerosol production, as well as an
164 under-estimation in the contribution of photochemically produced S/IVOC from photooxidized
165 “traditional” VOCs, due to partitioning of these low volatile compounds to chamber walls and

166 tubing (Krechmer et al., 2016; Ye et al., 2016; Liu et al., 2019). Accounting for this
167 under-estimation increases the predicted ASOA (Ma et al., 2017). The inclusion of these classes
168 of compounds have led to improvement in some urban SOA budget closure; however, many
169 studies still have indicated a general short-fall in ASOA budget even when including these
170 compounds from transportation-related emissions. (Dzepina et al., 2009; Tsimpidi et al., 2010;
171 Hayes et al., 2015; Cappa et al., 2016; Ma et al., 2017; McDonald et al., 2018).

172 Recent studies have indicated that emissions from volatile chemical products (VCPs),
173 defined as pesticides, coatings, inks, adhesives, personal care products, and cleaning agents
174 (McDonald et al., 2018), as well as cooking emissions (Hayes et al., 2015), asphalt emissions
175 (Khare et al., 2020), and solid fuel emissions from residential wood burning and/or cookstoves
176 (e.g., Hu et al., 2013, 2020; Schroder et al., 2018), are important. While total amounts of ASOA
177 precursors released in cities have dramatically declined (largely due to three-way catalytic
178 converters in cars (Warneke et al., 2012; Pollack et al., 2013; Zhao et al., 2017; Khare and
179 Gentner, 2018)), VCPs have not declined as quickly (Khare and Gentner, 2018; McDonald et al.,
180 2018). Besides a few cities in the US (Coggon et al., 2018; Khare and Gentner, 2018; McDonald
181 et al., 2018), extensive VCP emission quantification has not yet been published.

182 Due to the uncertainty on the emissions of ASOA precursors and on the amount of
183 ASOA formed from them, the number of premature deaths associated with urban organic
184 emissions is largely unknown. Since numerous studies have shown the importance of VCPs and
185 other non-traditional VOC emission sources, efforts have been made to try to improve the
186 representation and emissions of VCPs (Seltzer et al., 2021), which can reduce the uncertainty in
187 ASOA precursors and the associated premature deaths estimations. Currently, most studies have

188 not treated ASOA explicitly (e.g., Lelieveld et al., 2015; Silva et al., 2016; Ridley et al., 2018) in
189 source apportionment calculations of the premature deaths associated with long-term exposure of
190 $PM_{2.5}$. Most models represented total OA as non-volatile POA and “traditional” ASOA
191 precursors (transportation-based VOCs), which largely under-predict ASOA (Ensberg et al.,
192 2014; Hayes et al., 2015; Nault et al., 2018; Schroder et al., 2018) while over-predicting POA
193 (e.g., Hodzic et al., 2010b; Zhao et al., 2016a; Jathar et al., 2017). This does not reflect the
194 current understanding that POA is volatile and contributes to ASOA mass concentration (e.g.,
195 Grieshop et al., 2009; Lu et al., 2018). Though the models are estimating total OA correctly
196 (Ridley et al., 2018; Hodzic et al., 2020; Pai et al., 2020), the attribution of premature deaths to
197 POA instead of SOA formed from “traditional” and “non-traditional” sources, including IVOCs
198 from both sources, could lead to regulations that may not target the emissions that would reduce
199 OA in urban areas. As PM_1 and SOA mass are highest in urban areas (Fig. 1), also shown in
200 Jimenez et al. (2009), it is necessary to quantify the amount and identify the sources of ASOA to
201 target future emission standards that will optimally improve air quality and the associated health
202 impacts. As these emissions are from human activities, they will contribute to SOA mass outside
203 urban regions and to potential health impacts outside urban regions as well. Though there are
204 potentially other important exposure pathways to PM that may increase premature mortality,
205 such as exposure to solid-fuel emissions indoors (e.g., Kodros et al., 2018), the focus of this
206 paper is on exposure to outdoor ASOA and its associated impacts to premature mortality.

207 Here, we investigate the factors that control ASOA using 11 major urban, including
208 megacities, field studies (Fig. 1 and Table 1). The empirical relationships and numerical models
209 are then used to quantify the attribution of premature mortality to ASOA around the world, using

210 the observations to improve the modeled representation of ASOA. The results provide insight
211 into the importance of ASOA to global premature mortality due to $PM_{2.5}$ and further
212 understanding of the precursors and sources of ASOA in urban regions.

213

214 **2. Methods**

215 Here, we introduce the ambient observations from various campaigns used to constrain
216 ASOA production (Sect. 2.1), description of the simplified model used in CTMs to better predict
217 ASOA (Sect. 2.2), and description of how premature mortality was estimated for this study (Sect.
218 2.3). In the SI, the following can be found: description of the emissions used to calculate the
219 ASOA budget for five different locations (Sect. S1), description of how the ASOA budget was
220 calculated for the five different locations (Sect. S2), description of the CTM (GEOS-Chem) used
221 in this study (Sect. S3 - S4), and error analysis for the observations (Sect. S5).

222

223 **2.1 Ambient Observations**

224 For values not previously reported in the literature (Table S4), observations taken
225 between 11:00 – 16:00 local time were used to determine the slopes of SOA versus
226 formaldehyde (HCHO) (Fig. S1), peroxy acetyl nitrate (PAN) (Fig. S2), and O_x ($O_x = O_3 + NO_2$)
227 (Fig. S3). For CalNex, there was an approximate 48% difference between the two HCHO
228 measurements (Fig. S4). Therefore, the average between the two measurements were used in this
229 study, similar to what has been done in other studies for other gas-phase species (Bertram et al.,
230 2007). All linear fits, unless otherwise noted, use the orthogonal distance regression fitting
231 method (ODR).

232 For values in Table S4 through Table S8 not previously reported in the literature, the
 233 following procedure was applied to determine the emissions ratios, similar to the methods of
 234 Nault et al. (2018). An OH exposure ($OH_{exp} = [OH] \times \Delta t$), which is also the photochemical age
 235 (PA), was estimated by using the ratio of NO_x/NO_y (Eq. 1) or the ratio of
 236 m+p-xylene/ethylbenzene (Eq. 2). For the m+p-xylene/ethylbenzene, the emission ratio
 237 (Table S5) was determined by determining the average ratio during minimal photochemistry,
 238 similar to prior studies (de Gouw et al., 2017). This was done for only one study, TexAQS 2000.
 239 This method could be applied in that case as it was a ground campaign that operated both day
 240 and night; therefore, a ratio at night could be determined when there was minimal loss of both
 241 VOCs. The average emission ratio for the other VOCs was determined using Eq. 3 after the
 242 OH_{exp} was calculated in Eq. 1 or Eq. 2. The rate constants used for determining OH_{exp} and
 243 emission ratios are found in Table S12.

$$244 \quad OH_{exp} = [OH] \times t = \ln \left(\frac{\left(\frac{[NO_x]}{[NO_y]} \right)}{k_{OH+NO_2}} \right) \quad \text{Eq. 1}$$

$$245 \quad OH_{exp} = [OH] \times t = - \frac{1}{k_{m+p-xylene} - k_{ethylbenzene}} \times \ln \left(\frac{[m+p-xylene]_t}{[ethylbenzene]_t} - \frac{[m+p-xylene]_0}{[ethylbenzene]_0} \right) \quad \text{Eq. 2}$$

$$247 \quad \frac{[VOC(i)]}{[CO]}(0) = - \frac{[VOC(i)]}{[CO]}(t) \times \left(1 - \frac{1}{\exp(-k_i \times [OH]_{exp} \times t)} \right) \times k_i + \frac{[VOC(i)]}{[CO]}(t) \times k_i \quad \text{Eq. 3}$$

249
 250 **2.2 Updates to the SIMPLE Model**

251 With the combination of the new dataset, which expands across urban areas on three
252 continents, the SIMPLE parameterization for ASOA (Hodzic and Jimenez, 2011) is updated in
253 the standard GEOS-Chem model to reproduce observed ASOA in Fig. 2a. The parameterization
254 operates as represented by Eq. 4.



256 SOAP represents the lumped precursors of ASOA, k is the reaction rate coefficient with OH
257 ($1.25 \times 10^{-11} \text{ cm}^3 \text{ molecules}^{-1} \text{ s}^{-1}$), and $[\text{OH}]$ is the OH concentration in molecules cm^{-3} . This rate
258 constant is also consistent with observed ASOA formation time scale of ~ 1 day that has been
259 observed across numerous studies (e.g., de Gouw et al., 2005; DeCarlo et al., 2010; Hayes et al.,
260 2013; Nault et al., 2018; Schroder et al., 2018).

261 SOAP emissions were calculated based on the relationship between $\Delta\text{SOA}/\Delta\text{CO}$ and
262 $R_{\text{aromatics}}/\Delta\text{CO}$ in Fig. 2a. First, we calculated $R_{\text{aromatics}}/\Delta\text{CO}$ (Eq. 5) for each grid cell and time step
263 as follows:

$$264 \quad \frac{R_{\text{aromatics}}}{\Delta\text{CO}} = \frac{E_{\text{B}} \times k_{\text{B}} + E_{\text{T}} \times k_{\text{T}} + E_{\text{X}} \times k_{\text{X}}}{E_{\text{CO}}} \quad \text{Eq. 5}$$

265 Where E and k stand for the emission rate and reaction rate coefficient with OH, respectively, for
266 benzene (B), toluene (T), and xylenes (X). Ethylbenzene was not included in this calculation
267 because its emission was not available in HTAPv2 emission inventory. However, ethylbenzene
268 contributed a minor fraction of the mixing ratio ($\sim 7\%$, Table S5) and reactivity ($\sim 6\%$) of the
269 total BTEX across the campaigns. Reaction rate constants used in this study were 1.22×10^{-12} ,
270 5.63×10^{-12} , and $1.72 \times 10^{-11} \text{ cm}^3 \text{ molec.}^{-1} \text{ s}^{-1}$ for benzene, toluene, and xylene, respectively
271 (Atkinson and Arey, 2003; Atkinson et al., 2006). The $R_{\text{aromatics}}/\Delta\text{CO}$ allows a dynamic

272 calculation of the $E(\text{VOC})/E(\text{CO}) = \text{SOA}/\Delta\text{CO}$. Hodzic and Jimenez (2011) and Hayes et al.
 273 (2015) used a constant value of 0.069 g g^{-1} , which worked well for the two cities investigated,
 274 but not for the expanded dataset studied here. Thus, both the aromatic emissions and CO
 275 emissions are used in this study to better represent the variable emissions of ASOA precursors
 276 (Fig. S5).

277 Second, $E_{\text{SOAP}}/E_{\text{CO}}$ can be obtained from the result of Eq. 6, using slope and intercept in
 278 Fig. 2a, with a correction factor (F) to consider additional SOA production after 0.5 PA
 279 equivalent days, since Fig. 2a shows the comparison at 0.5 PA equivalent days.

$$280 \quad \frac{E_{\text{SOAP}}}{E_{\text{CO}}} = \left(\text{Slope} \times \frac{R_{\text{Aromatics}}}{\Delta\text{CO}} + \text{Intercept} \right) \times F \quad \text{Eq. 6}$$

281 Where slope is 24.8 and intercept is -1.7 from Fig. 2a. F (Eq. 7) can be calculated as follows:

$$282 \quad F = \frac{ASOA_{t=\infty}}{ASOA_{t=0.5d}} = \frac{SOAP_{t=0}}{SOAP_{t=0} \times (1 - \exp(-k \times \Delta t \times [\text{OH}])), \Delta t = 43200 \text{ s}} \quad \text{Eq. 7}$$

283 F was calculated as 1.8 by using $[\text{OH}] = 1.5 \times 10^6 \text{ molecules cm}^{-3}$, which was used in the
 284 definition of 0.5 PA equivalent days for Fig. 2a.

285 Finally, E_{SOAP} can be computed by multiplying CO emissions (E_{CO}) for every grid point
 286 and time step in GEOS-Chem by the $E_{\text{SOAP}}/E_{\text{CO}}$ ratio.

287

288 **2.3 Estimation of Premature Mortality Attribution**

289 Premature deaths were calculated for five disease categories: ischemic heart disease
 290 (IHD), stroke, chronic obstructive pulmonary disease (COPD), acute lower respiratory illness
 291 (ALRI), and lung cancer (LC). We calculated premature mortality for the population aged more
 292 than 30 years, using Eq. 8.

293
$$Premature\ Death = Pop \times y_0 \times \frac{RR - 1}{RR}$$
 Eq. 8

294 Mortality rate, y_0 , varies according to the particular disease category and geographic region,
 295 which is available from Global Burden of Disease (GBD) Study 2015 database (IHME, 2016).
 296 Population (Pop) was obtained from Columbia University Center for International Earth Science
 297 Information Network (CIESIN) for 2010 (CIESIN, 2017). Relative risk, RR, can be calculated as
 298 shown in Eq. 9.

299
$$RR = 1 + \alpha \times \left(1 - \exp\left(\beta \times \left(PM_{2.5} - PM_{2.5,Threshold}\right)^\rho\right)\right)$$
 Eq. 9

300 α , β , and ρ values depend on disease category and are calculated from Burnett et al. (2014) (see
 301 Table S14 and associated file). If the $PM_{2.5}$ concentrations are below the $PM_{2.5}$ threshold value
 302 (Table S14), premature deaths were computed as zero. However, there could be some health
 303 impacts at concentrations below the $PM_{2.5}$ threshold values (Krewski et al., 2009); following the
 304 methods of the GBD studies, these can be viewed as lower bounds on estimates of premature
 305 deaths.

306 We performed an additional sensitivity analysis using the Global Exposure Mortality
 307 Model (GEMM) (Burnett et al., 2018). For the GEMM analysis, we also used age stratified
 308 population data from GWPv3. Premature death is calculated the same as shown in Eq. 8;
 309 however, the relative risk differs. For the GEMM model, the relative risk can be calculated as
 310 shown in Eq. 10.

311
$$RR = \exp(\theta \times \lambda) \text{ with } \lambda = \frac{\log\left(1 + \frac{z}{\alpha}\right)}{\left(1 + \exp\left(\frac{(\hat{\mu} - z)}{\pi}\right)\right)}$$
 Eq. 10

312 Here $z = \max(0, PM_{2.5} - PM_{2.5, Threshold})$; θ , π , $\hat{\mu}$, α , and $PM_{2.5, Threshold}$ depends on disease category and
313 are from Burnett et al. (2018). Similar to the Eq. 9, if the concentrations are below the threshold
314 ($2.4 \mu\text{g m}^{-3}$, Burnett et al. (2018)), then premature deaths are computed as zero; however, the
315 GEMM has a lower threshold than the GBD method.

316 For GBD, we do not consider age-specific mortality rates or risks. For GEMM, we
317 calculate age-specific health impacts with age-specific parameters in the exposure response
318 function (Table S15). We combine the age-specific results of the exposure-response function
319 with age distributed population data from GPW (CIESIN, 2017) and a national mortality rate
320 across all ages to assess age-specific mortality.

321 We calculated total premature deaths using annual average total $PM_{2.5}$ concentrations
322 derived from satellite-based estimates at the resolution of $0.1^\circ \times 0.1^\circ$ from van Donkelaar et al.
323 (2016) . Application of the remote-sensing based $PM_{2.5}$ at the $0.1^\circ \times 0.1^\circ$ resolution rather than
324 direct use of the GEOS-Chem model concentrations at the $2^\circ \times 2.5^\circ$ resolution helps reduce
325 uncertainties in the quantification of $PM_{2.5}$ exposure inherent in coarser estimates (Punger and
326 West, 2013). We also calculated deaths by subtracting from this amount the total annual average
327 ASOA concentrations derived from GEOS-Chem (Fig. S11). To reduce uncertainties related to
328 spatial gradients and total concentration magnitudes in our GEOS-Chem simulations of $PM_{2.5}$,
329 our modeled ASOA was calculated as the fraction of ASOA to total $PM_{2.5}$ in GEOS-Chem,
330 multiplied by the satellite-based $PM_{2.5}$ concentrations (Eq. 11).

$$331 \quad ASOA_{sat} = (ASOA_{mod} / PM_{2.5, mod}) \times PM_{2.5, sat} \quad \text{Eq. 11}$$

332 Finally, this process for estimating $PM_{2.5}$ health impacts considers only $PM_{2.5}$ mass concentration
333 and does not distinguish toxicity by composition, consistent with the current US EPA position
334 expressed in Sacks et al. (2019).

335

336 **3. Observations of ASOA Production across Three Continents**

337 **3.1 Observational Constraints of ASOA Production across Three Continents**

338 Measurements during intensive field campaigns in large urban areas better constrain
339 concentrations and atmospheric formation of ASOA because the scale of ASOA enhancement is
340 large compared to SOA from a regional background. Generally, ASOA increased with the
341 amount of urban precursor VOCs and with atmospheric PA (de Gouw et al., 2005; de Gouw and
342 Jimenez, 2009; DeCarlo et al., 2010; Hayes et al., 2013; Nault et al., 2018; Schroder et al., 2018;
343 Shah et al., 2018). In addition, ASOA correlates strongly with gas-phase secondary
344 photochemical species, including O_x , HCHO, and PAN (Herndon et al., 2008; Wood et al., 2010;
345 Hayes et al., 2013; Zhang et al., 2015; Nault et al., 2018; Liao et al., 2019) (Table S4; Fig. S1 to
346 Fig. S3), which are indicators of photochemical processing of emissions.

347 However, as initially discussed by Nault et al. (2018) and shown in Fig. 3, there is large
348 variability in these various metrics across the urban areas evaluated here. To the best of the
349 authors' knowledge, this variability has not been explored and its physical meaning has not been
350 interpreted. As shown in Fig. 3, though, the trends in $\Delta SOA/\Delta CO$ are similar to the trends in the
351 slopes of SOA versus O_x , PAN, or HCHO. For example, Seoul is the highest for nearly all
352 metrics, and is approximately a factor of 6 higher than the urban area, Houston, that generally

353 showed the lowest photochemical metrics. This suggests that the variability is related to a
354 physical factor, including emissions and chemistry.

355 The VOC concentration, together with how quickly the emitted VOCs react ($\sum k_i \times [\text{VOC}]_i$,
356 i.e., the hydroxyl radical, or OH, reactivity of VOCs), where k is the OH rate coefficient for each
357 VOC, are a determining parameter for ASOA formation over urban spatial scales (Eq. 12).
358 ASOA formation is normalized here to the excess CO mixing ratio (ΔCO) to account for the
359 effects of meteorology, dilution, and non-urban background levels, and allow for easier
360 comparison between different studies:

$$361 \quad \frac{\Delta \text{ASOA}}{\Delta \text{CO}} \propto [\text{OH}] \times \Delta t \times \left(\sum_i k_i \times \left[\frac{\text{VOC}}{\text{CO}} \right]_i \times Y_i \right) \quad \text{Eq. 12}$$

362 where Y is the aerosol yield for each compound (mass of SOA formed per unit mass of precursor
363 reacted), and $[\text{OH}] \times \Delta t$ is the PA.

364 BTEX are one group of known ASOA precursors (Gentner et al., 2012; Hayes et al.,
365 2013), and their emission ratio (to CO) was determined for all campaigns (Table S5). BTEX can
366 thus provide insight into ASOA production. Fig. 2a shows that the variation in ASOA (at PA =
367 0.5 equivalent days) is highly correlated with the emission reactivity ratio of BTEX (R_{BTEX} ,
368 $\sum_i [\text{VOC}/\text{CO}]_i$) across all the studies. However, BTEX alone cannot account for much of the
369 ASOA formation (see budget closure discussion below), and instead, BTEX may be better
370 thought of as both partial contributors and also as indicators for the co-emission of other
371 (unmeasured) organic precursors that are also efficient at forming ASOA.

372 O_x , PAN, and HCHO are produced from the oxidation of a much wider set of VOC
373 precursors (including small alkenes, which do not appreciably produce SOA when oxidized).

374 These alkenes have similar reaction rate constants with OH as the most reactive BTEX
375 compounds (Table S12); however, their emissions and concentration can be higher than BTEX
376 (Table S7). Thus, alkenes would dominate R_{Total} , leading to O_x , HCHO, and PAN being produced
377 more rapidly than ASOA (Fig. 2b–d). When R_{BTEX} becomes more important for R_{Total} , the emitted
378 VOCs are more efficient in producing ASOA. Thus, the ratio of ASOA to gas-phase
379 photochemical products shows a strong correlation with $R_{\text{BTEX}}/R_{\text{Total}}$ (Fig. 2b–d).

380 An important aspect of this study is that most of these observations occurred during
381 spring and summer, when solid fuel emissions are expected to be lower (e.g., Chafe et al., 2015;
382 Lam et al., 2017; Hu et al., 2020). Further, the most important observations used here are during
383 the afternoon, investigating specifically the photochemically produced ASOA. These results here
384 might partially miss any ASOA produced through nighttime aqueous chemistry or oxidation by
385 nitrate radical (Kodros et al., 2020). However, two of the studies included in our analysis,
386 Chinese Outflow (CAPTAIN, 2011) and New York City (WINTER, 2015), occurred in late
387 winter/early spring, when solid fuel emissions were important (Hu et al., 2013; Schroder et al.,
388 2018). We find that these observations lie within the uncertainty in the slope between ASOA and
389 R_{BTEX} (Fig. 2a). Their photochemically produced ASOA observed under strong impact from solid
390 fuel emissions shows similar behavior as the ASOA observed during spring and summer time.
391 Thus, given the limited datasets currently available, photochemically produced ASOA is
392 expected to follow the relationship shown in Fig. 2a and is expected to also follow this
393 relationship for regions impacted by solid fuel burning. Future comprehensive studies in regions
394 strongly impacted by solid fuel burning are needed to further investigate photochemical ASOA
395 production under those conditions.

396

397 **3.2 Budget Closure of ASOA for 4 Urban Areas on 3 Continents Indicates Reasonable** 398 **Understanding of ASOA Sources**

399 To investigate the correlation between ASOA and R_{BTEX} , a box model using the emission
400 ratios from BTEX (Table S5), other aromatics (Table S8), IVOCs (Sect. S1), and SVOCs (Sect.
401 S1) was run for five urban areas: New York City, 2002, Los Angeles, Beijing, London, and New
402 York City, 2015 (see Sect. S1 and S3 for more information). The differences in the results shown
403 in Fig. 4 are due to differences in the emissions for each city. We show that BTEX alone cannot
404 explain the observed ASOA budget for urban areas around the world. Fig. 4a shows that
405 approximately $25 \pm 6\%$ of the observed ASOA originates from the photooxidation of BTEX.
406 BTEX only explaining 25% of the observed ASOA is similar to prior studies that have done
407 budget analysis of precursor gases and observed SOA (e.g., Dzepina et al., 2009; Ensberg et al.,
408 2014; Hayes et al., 2015; Ma et al., 2017; Nault et al., 2018). Therefore, other precursors must
409 account for most of the ASOA produced.

410 Because alkanes, alkenes, and oxygenated compounds with carbon numbers less than 6
411 are not significant ASOA precursors, we focus on emissions and sources of BTEX, other
412 mono-aromatics, IVOCs, and SVOCs. These three classes of VOCs, aromatics, IVOCs, and
413 SVOCs, have been suggested to be significant ASOA precursors in urban atmospheres
414 (Robinson et al., 2007; Hayes et al., 2015; Ma et al., 2017; McDonald et al., 2018; Nault et al.,
415 2018; Schroder et al., 2018; Shah et al., 2018), originating from both fossil fuel and VCP
416 emissions.

417 Using the best available emission inventories from cities on three continents
418 (EMEP/EEA, 2016; McDonald et al., 2018; Li et al., 2019) and observations, we quantify the
419 emissions of BTEX, other mono-aromatics, IVOCs, and SVOCs for both fossil fuel (e.g.,
420 gasoline, diesel, kerosene, etc.), VCPs (e.g., coatings, inks, adhesives, personal care products,
421 and cleaning agents), and cooking sources (Fig. 5). This builds off the work of McDonald et al.
422 (2018) for urban regions on three different continents.

423 Note, the emissions investigated here ignore any oxygenated VOC emissions not
424 associated with IVOCs and SVOCs due to the challenge in estimating the emission ratios for
425 these compounds (de Gouw et al., 2018). Further, SVOC emission ratios are estimated from the
426 average POA observed by the AMS during the specific campaign and scaled by profiles in
427 literature for a given average temperature and average OA (Robinson et al., 2007; Worton et al.,
428 2014; Lu et al., 2018). As most of the campaigns had an average OA between 1 and 10 $\mu\text{g m}^{-3}$
429 and temperature of ~ 298 K, this led to the majority of the estimated emitted SVOC gases in the
430 highest SVOC bin. However, as discussed later, this does not lead to SVOCs dominating the
431 predicted ASOA due to taking into account the fragmentation and overall yield from the
432 photooxidation of SVOC to ASOA.

433 Combining these inventories and observations for the various locations provide the
434 following insights about the potential ASOA precursors not easily measured or quantified in
435 urban environments (e.g., Zhao et al., 2014; Lu et al., 2018): (1) aromatics from fossil fuel
436 accounts for 14-40% (mean 22%) of the total BTEX and IVOC emissions for the five urban
437 areas investigated in-depth (Fig. 5), agreeing with prior studies that have shown that the observed
438 ASOA cannot be reconciled by the observations or emission inventory of aromatics from fossil

439 fuels (e.g., Ensberg et al., 2014; Hayes et al., 2015). (2) BTEX from both fossil fuels and VCPs
440 account for 25-95% (mean 43%) of BTEX and IVOC emissions (Fig. 5). China has the lowest
441 contribution of IVOCs, potentially due to differences in chemical make-up of the solvents used
442 daily (Li et al., 2019), but more research is needed to investigate the differences in IVOCs:BTEX
443 from Beijing versus US and UK emission inventories. Nonetheless, this shows the importance of
444 IVOCs for both emissions and ASOA precursors. (3) IVOCs are generally equal to, if not greater
445 than, the emissions of BTEX in 4 of the 5 urban areas investigated here (Fig. 5). (4) Overall,
446 VCPs account for a large fraction of the BTEX and IVOC emissions for all five cities. (5)
447 Finally, SVOCs account for 27-88% (mean 53%) of VOCs generally considered ASOA
448 precursors (VOCs with volatility saturation concentrations $\leq 10^7 \mu\text{g m}^{-3}$) (Fig. S6). Beijing has
449 the highest contribution of SVOCs to ASOA precursors due to the use of solid fuels and cooking
450 emissions (Hu et al., 2016). Also, this indicates the large contribution of a class of VOCs
451 difficult to measure (Robinson et al., 2007) that are an important ASOA precursor (e.g., Hayes et
452 al., 2015), showing further emphasis should be placed in quantifying the emissions of this class
453 of compounds.

454 These results provide an ability to further investigate the mass balance of predicted and
455 observed ASOA for these urban locations (Fig. 4). The inclusion of IVOCs, other aromatics not
456 including BTEX, and SVOCs leads to the ability to explain, on average, $85\pm 12\%$ of the observed
457 ASOA for these urban locations around the world (Fig. 4a). Further, VCP contribution to ASOA
458 is important for all these urban locations, accounting for, on average, $37\pm 3\%$ of the observed
459 ASOA (Fig. 4b).

460 This bottom-up mass budget analysis provides important insights to further explain the
461 correlation observed in Fig. 2. First, IVOCs are generally co-emitted from similar sources as
462 BTEX for the urban areas investigated in-depth (Fig. 5). The oxidation of these co-emitted
463 species leads to the ASOA production observed across the urban areas around the world. Second,
464 S/IVOCs generally have similar rate constants as toluene and xylenes ($\geq 1 \times 10^{-11} \text{ cm}^3 \text{ molec.}^{-1} \text{ s}^{-1}$)
465 (Zhao et al., 2014, 2017), the compounds that contribute the most to R_{BTEX} , explaining the rapid
466 ASOA production that has been observed in various studies (de Gouw and Jimenez, 2009;
467 DeCarlo et al., 2010; Hayes et al., 2013; Hu et al., 2013, 2016; Nault et al., 2018; Schroder et al.,
468 2018) and correlation (Fig. 2). Finally, the contribution of VCPs and fossil fuel sources to ASOA
469 is similar across the cities, expanding upon and further supporting the conclusion of McDonald
470 et al. (2018) in the importance of identifying and understanding VCP emissions in order to
471 explain ASOA.

472 This investigation shows that the bottom-up calculated ASOA agrees with observed
473 top-down ASOA within 15%. As highlighted above, this ratio is explained by the co-emissions
474 of IVOCs with BTEX from traditional sources (diesel, gasoline, and other fossil fuel emissions)
475 and VCPs (Fig. 5) along with similar rate constants for these ASOA precursors (Table S12).
476 Thus, the $\text{ASOA}/R_{\text{BTEX}}$ ratio obtained from Fig. 2 results in accurate predictions of ASOA for the
477 urban areas evaluated here, and this value can be used to better estimate ASOA with chemical
478 transport models (Sect. 4).

479

480 **4. Improved Urban SIMPLE Model Using Multi-Cities to Constrain**

481 The SIMPLE model was originally designed and tested against the observations collected
482 around Mexico City (Hodzic and Jimenez, 2011). It was then tested against observations
483 collected in Los Angeles (Hayes et al., 2015; Ma et al., 2017). As both data sets have nearly
484 identical $\Delta\text{SOA}/\Delta\text{CO}$ and R_{BTEX} (Fig. 2 and Fig. 3), it is not surprising that the SIMPLE model
485 did well in predicting the observed $\Delta\text{SOA}/\Delta\text{CO}$ for these two urban regions with consistent
486 parameters. Though the SIMPLE model generally performed better than more explicit models, it
487 generally had lower skill in predicting the observed ASOA in urban regions outside of Mexico
488 City and Los Angeles (Shah et al., 2019; Pai et al., 2020).

489 This may stem from the original SIMPLE model with constant parameters missing the
490 ability to change the amount and reactivity of the emissions, which are different for the various
491 urban regions, versus the ASOA precursors being emitted proportionally to only CO (Hodzic and
492 Jimenez, 2011; Hayes et al., 2015). For example, in the HTAP emissions inventory, the CO
493 emissions for Seoul, Los Angeles, and Mexico City are all similar (Fig. S8); thus, the original
494 SIMPLE model would suggest similar $\Delta\text{SOA}/\Delta\text{CO}$ for all three urban locations. However, as
495 shown in Fig. 2 and Fig. 3, the $\Delta\text{SOA}/\Delta\text{CO}$ is different by nearly a factor of 2. The inclusion of
496 the emissions and reactivity, where R_{BTEX} for Seoul is approximately a factor of 2.5 higher than
497 Los Angeles and Seoul, into the improved SIMPLE model better accounts for the variability in
498 SOA production, as shown in Fig. 2. Thus, the inclusion and use of this improved SIMPLE
499 model refines the simplified representation of ASOA in chemical transport models and/or box
500 models.

501 The “improved” SIMPLE shows higher ASOA compared to the default VBS
502 GEOS-Chem (Fig. 6a,b). In areas strongly impacted by urban emissions (e.g., Europe, East Asia,

503 India, east and west coast US, and regions impacted by Santiago, Chile, Buenos Aires,
504 Argentina, Sao Paulo, Brazil, Durban and Cape Town, South Africa, and Melbourne and Sydney,
505 Australia), the “improved” SIMPLE model predicts up to $14 \mu\text{g m}^{-3}$ more ASOA, or ~30 to 60
506 times more ASOA than the default scheme (Fig. 6c,d). As shown in Fig. 1, during intensive
507 measurements, the ASOA composed 17-39% of PM_{10} , with an average contribution of ~25%. The
508 default ASOA scheme in GEOS-Chem greatly underestimates the fractional contribution of
509 ASOA to total $\text{PM}_{2.5}$ (<2%; Fig. 6e). The “improved” SIMPLE model greatly improves the
510 predicted fractional contribution, showing that ASOA in the urban regions ranges from 15-30%,
511 with an average of ~15% for the grid cells corresponding to the urban areas investigated here
512 (Fig. 6f). Thus, the “improved” SIMPLE predicts the fractional contribution of ASOA to total
513 $\text{PM}_{2.5}$ far more realistically, compared to observations. As discussed in Sect. 2.3 and Eq. 11,
514 having the model accurately predict the fractional contribution of ASOA to the total PM is very
515 important, as the total $\text{PM}_{2.5}$ is derived from satellite-based estimates (van Donkelaar et al.,
516 2015), and the model fractions are then applied to those total $\text{PM}_{2.5}$ estimates. The ability for the
517 “improved” SIMPLE model to better represent the ASOA composition provides confidence
518 attributing the ASOA contribution to premature mortality.

519

520 **5. Preliminary Evaluation of Worldwide Premature Deaths Due to ASOA with Updated** 521 **SIMPLE Parameterization**

522 The improved SIMPLE parameterization is used along with GEOS-Chem to provide an
523 accurate estimation of ASOA formation in urban areas worldwide and provide an ability to
524 obtain realistic simulations of ASOA based on measurement data. We use this model to quantify

525 the attribution of $PM_{2.5}$ ASOA to premature deaths. Analysis up to this point has been for PM_1 ;
526 however, both the chemical transport model and epidemiological studies utilize $PM_{2.5}$. For
527 ASOA, this will not impact the discussion and results here because the mass of OA (typically
528 80–90%) is dominated by PM_1 (e.g., Bae et al., 2006; Seinfeld and Pandis, 2006), and ASOA is
529 formed mostly through condensation of oxidized species, which favors partitioning onto smaller
530 particles (Seinfeld and Pandis, 2006).

531 The procedure for this analysis is described in Fig. 7 and Sect. 2.3 and S3. Briefly, we
532 combine high-resolution satellite-based $PM_{2.5}$ estimates (for exposure) and a chemical transport
533 model (GEOS-Chem, for fractional composition) to estimate ASOA concentrations and various
534 sensitivity analysis (van Donkelaar et al., 2015). We calculated ~3.3 million premature deaths
535 (using the Integrated Exposure-Response, IER, function) are due to long-term exposure of
536 ambient $PM_{2.5}$ (Fig. S9, Table S16), consistent with recent literature (Cohen et al., 2017).

537 The attribution of ASOA $PM_{2.5}$ premature deaths can be calculated one of two ways: (a)
538 marginal method (Silva et al., 2016) or (b) attributable fraction method (Anenberg et al., 2019).
539 For method (a), it is assumed that a fraction of the ASOA is removed, keeping the rest of the
540 $PM_{2.5}$ components approximately constant, and the change in deaths is calculated from the deaths
541 associated with the total concentration less the deaths calculated using the reduced total $PM_{2.5}$
542 concentrations. For method (b), the health impact is attributed to each $PM_{2.5}$ component by
543 multiplying the total deaths by the fractional contribution of each component to total $PM_{2.5}$. For
544 method (a), the deaths attributed to ASOA are ~340,000 people per year (Fig. 8); whereas, for
545 method (b), the deaths are ~370,000 people per year. Both of these are based on the IER response
546 function (Cohen et al., 2017).

547 Additional recent work (Burnett et al., 2018) has suggested less reduction in the
548 premature deaths versus $PM_{2.5}$ concentration relationship at higher $PM_{2.5}$ concentrations, and
549 lower concentration limits for the threshold below which this relationship is negligible, both of
550 which lead to much higher estimates of $PM_{2.5}$ associated premature deaths. This is generally
551 termed the Global Exposure Mortality Model (GEMM). Using the two attribution methods
552 described above (a and b), the ASOA $PM_{2.5}$ premature deaths are estimated to be ~640,000
553 (method a) and ~900,000 (method b) (Fig. S9 and Fig. S12 and Table S17).

554 Compared to prior studies using chemical transport models to estimate premature deaths
555 associated with ASOA (e.g., Silva et al., 2016; Ridley et al., 2018), which assumed non-volatile
556 POA and “traditional” ASOA precursors, the attribution of premature mortality due to ASOA is
557 over an order of magnitude higher in this study (Fig. 9). This occurs using either the IER and
558 GEMM approach for estimating premature mortality (Fig. 9). For regions with larger populations
559 and more $PM_{2.5}$ pollution, the attribution is between a factor of 40 to 80 higher. This stems from
560 the non-volatile POA and “traditional” ASOA precursors over-estimating POA and
561 under-estimating ASOA compared to observations (Schroder et al., 2018). These offsetting
562 errors will lead to model predicted total OA similar to observations (Ridley et al., 2018; Schroder
563 et al., 2018), yet different conclusions on whether POA versus SOA is more important for
564 reducing $PM_{2.5}$ associated premature mortality. Using a model constrained to day-time
565 atmospheric observations (Fig. 2 and Fig. 4, see Sect. 4) leads to a more accurate than earlier
566 estimation of the contribution of photochemically-produced ASOA to $PM_{2.5}$ associated
567 premature mortality that has not been possible in prior studies. We note that ozone concentrations
568 change little as we change the ASOA simulation (see Sect. S4 and Fig. S14).

569 A limitation in this study is the lack of sufficient measurements in South and Southeast
570 Asia, Eastern Europe, Africa, and South America (Fig. 1), though these areas account for 44% of
571 the predicted reduction in premature mortality for the world (Table S16). However, as
572 highlighted in Table S18, these regions likely still consume both transportation fuels and VCPs,
573 although in lower per capita amounts than more industrialized countries. This consumption is
574 expected to lead to the same types of emissions as for the cities studied here, though more field
575 measurements are needed to validate global inventories of VOCs and resulting oxidation
576 products in the developing world. Transportation emissions of VOCs are expected to be more
577 dominant in the developing world due to higher VOC emission factors associated with inefficient
578 combustion engines, such as two-stroke scooters (Platt et al., 2014) and auto-rickshaws (e.g.,
579 Goel and Guttikunda, 2015).

580 Solid fuels are used for residential heating and cooking, which impact the outdoor air
581 quality as well (Hu et al., 2013, 2016; Lacey et al., 2017; Stewart et al., 2020), and which also
582 lead to SOA (Heringa et al., 2011). As discussed in Sect. 3.1, though the majority of the studies
583 evaluated here occurred in spring to summer time, when solid fuel emissions are decreased, two
584 studies occurred during the winter/early spring time, where solid fuel emissions were important
585 (Hu et al., 2013; Schroder et al., 2018). These studies still follow the same relationship between
586 ASOA and R_{BTEX} as the studies that focused on spring/summer time photochemistry. Thus, the
587 limited datasets available indicate that photochemically produced ASOA from solid fuels follow
588 a similar relationship to that from other ASOA sources.

589 Also, solid fuel sources are included in the inventories used in our modeling. For the
590 HTAP emission inventory used here (Janssens-Maenhout et al., 2015), small-scale combustion,

591 which includes heating and cooking (e.g., solid-fuel use), is included in the residential emission
592 sector. Both CO and BTEX are included in this source, and can account for a large fraction of the
593 total emissions where solid-fuel use may be important (Fig. S15). Thus, as CO and BTEX are
594 used in the updated SIMPLE model, and campaigns that observed solid-fuel emissions fall
595 within the trend for all urban areas, the solid-fuel contribution to photochemically-produced
596 ASOA is accounted for (as accurately as allowed by current datasets) in the estimation of ASOA
597 for the attribution to premature mortality.

598 Note that recent work has observed potential nighttime aqueous chemistry and/or
599 oxidation by nitrate radical from solid fuel emissions to produce ASOA (Kodros et al., 2020).
600 Thus, missing this source of ASOA may lead to an underestimation of total ASOA versus the
601 photochemically-produced ASOA we discuss here, leading to a potential underestimation in the
602 attribution of ASOA to premature mortality. From the studies that investigated “night-time
603 aging” of solid-fuel emissions to form SOA, we predict that the total ASOA may be
604 underestimated by 1 to 3 $\mu\text{g m}^{-3}$ (Kodros et al., 2020). This potential underestimation, though, is
605 less than the current underestimation in ASOA in GEOS-Chem (default versus “Updated”
606 SIMPLE).

607 Recently, emission factors from Abidjan, Côte d’Ivoire, a developing urban area, showed
608 the dominance of emissions from transportation and solid fuel burning, with BTEX being an
609 important fraction of the total emissions, and that all the emissions were efficient in producing
610 ASOA (Dominutti et al., 2019). Further, investigation of emissions in New Delhi region of India
611 demonstrated the importance of both transportation and solid fuel emissions (Stewart et al.,
612 2020; Wang et al., 2020) while model comparisons with observations show an underestimation

613 of OA compared to observations due to a combination of emissions and OA representation (Jena
614 et al., 2020). Despite emission source differences, SOA is still an important component of $PM_{2.5}$
615 (e.g., Singh et al., 2019) and thus will impact air quality and premature mortality in developing
616 regions. Admittedly, though, our estimates will be less accurate for these regions.

617

618 **6. Conclusions**

619 In summary, ASOA is an important, though inadequately constrained component of air
620 pollution in megacities and urban areas around the world. This stems from the complexity
621 associated with the numerous precursor emission sources, chemical reactions, and oxidation
622 products that lead to observed ASOA concentrations. We have shown here that the variability in
623 observed ASOA across urban areas is correlated with R_{BTEX} , a marker for the co-emissions of
624 IVOC from both transportation and VCP emissions. Global simulations indicate ASOA
625 contributes to a substantial fraction of the premature mortality associated with $PM_{2.5}$. Reductions
626 of the ASOA precursors will reduce the premature deaths associated with $PM_{2.5}$, indicating the
627 importance of identifying and reducing exposure to sources of ASOA. These sources include
628 emissions that are both traditional (transportation) as well as non-traditional emissions of
629 emerging importance (VCPs) to ambient $PM_{2.5}$ concentrations in cities around the world. Further
630 investigation of speciated IVOCs and SVOCs for urban areas around the world along with SOA
631 mass concentration and other photochemical products (e.g., O_x , PAN, and HCHO) for other
632 urban areas, especially in South Asia, throughout Africa, and throughout South America, would
633 provide further constraints to improve the SIMPLE model and our understanding of the emission
634 sources and chemistry that leads to the observed SOA and its impact on premature mortality.

635 Acknowledgements

636

637 This study was partially supported by grants from NASA NNX15AT96G, NNX16AQ26G, Sloan
638 Foundation 2016-7173, NSF AGS-1822664, EPA STAR 83587701-0, NERC NE/H003510/1,
639 NERC NE/H003177/1, NERC NE/H003223/1, NOAA NA17OAR4320101, NCAS
640 R8/H12/83/037, Natural Science and Engineering Research Council of Canada (NSERC,
641 RGPIN/05002-2014), and the Fonds de Recherche du Québec —Nature et technologies
642 (FRQNT, 2016-PR-192364). This manuscript has not been formally reviewed by EPA. The
643 views expressed in this document are solely those of the authors and do not necessarily reflect
644 those of the Agency. EPA does not endorse any products or commercial services mentioned in
645 this publication. We thank Katherine Travis for useful discussions. We acknowledge B J. Bandy,
646 J. Lee, G. P. Mills, d. D. Montzka, J. Stutz, A. J. Weinheimer E. J. Williams, E. C. Wood, and D.
647 R. Worsnop for use of their data.

648

649 Data Availability

650 TexAQS measurements are available at
651 <https://esrl.noaa.gov/csl/groups/csl7/measurements/2000TexAQS/LaPorte/DataDownload/> and
652 upon request. NEAQS measurements are available at
653 <https://www.esrl.noaa.gov/csl/groups/csl7/measurements/2002NEAQS/>. MILAGRO
654 measurements are available at <http://doi.org/10.5067/Aircraft/INTEXB/Aerosol-TraceGas>.
655 CalNex measurements are available at
656 <https://esrl.noaa.gov/csl/groups/csl7/measurements/2010calnex/Ground/DataDownload/>.
657 ClearfLo measurements are available at
658 <https://catalogue.ceda.ac.uk/uuid/6a5f9eedd68f43348692b3bace3eba45>. SEAC⁴RS measurements
659 are available at <http://doi.org/10.5067/Aircraft/SEAC4RS/Aerosol-TraceGas-Cloud>. WINTER
660 measurements are available at https://data.eol.ucar.edu/master_lists/generated/winter/.
661 KORUS-AQ measurements are available at
662 <http://doi.org/10.5067/Suborbital/KORUSAQ/DATA01>. Data from Chinese campaigns are
663 available upon request, and rest of data used were located in papers cited. GEOS-Chem data
664 available upon request. Figures will become accessible at
665 cires1.colorado.edu/jimenez/group_pubs.html.

666

667 Competing Interests

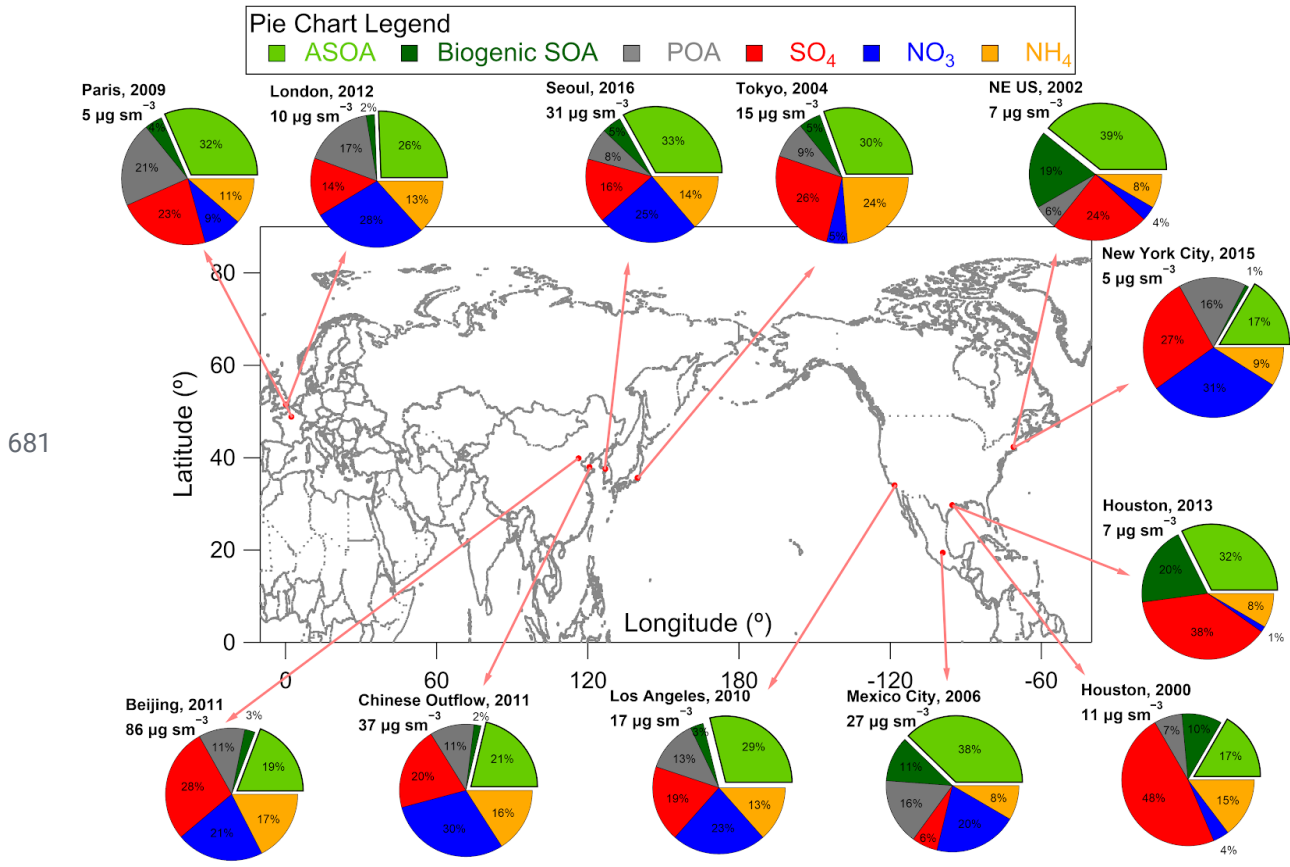
668 The authors declare no competing interests.

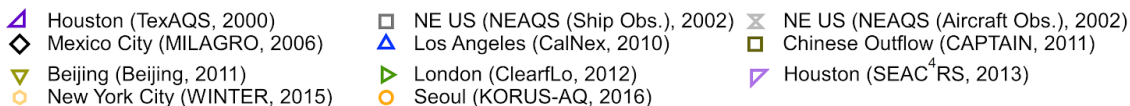
669

670 Author Contribution

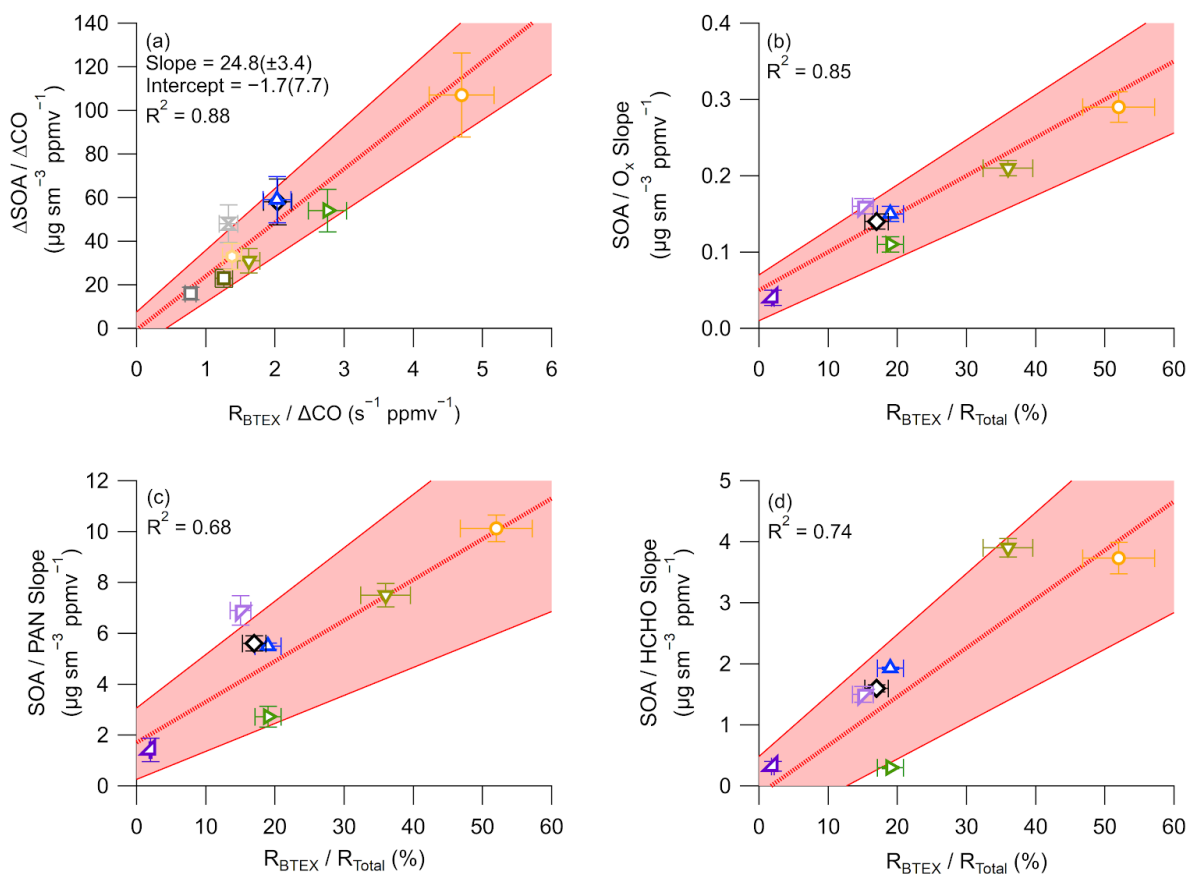
671 B.A.N., D.S.J., B.C.M., J.A.dG., and J.L.J designed the experiment and wrote the paper. B.A.N.,
672 PC.-J., D.A.D., W.H., J.C.S, J.A., D.R.B., M.R.C., H.C., M.M.C., P.F.D, G.S.D., R.D., F.F, A.F.,
673 J.B.G., G.G., J.F.H, T.F.H., P.L.H., J.H., M.H., L.G.H., B.T.J., W.C.K., J.L., I.B.P., J.P., B.R.,

674 C.E.R., D.R., J.M.R., T.B.R, M.S., J.W., C.W., P.W., G.M.W., D.E.Y., B.Y., J.A.dG., and J.L.J.
675 collected and analyzed the data. D.S.J. and A.H. ran the GEOS-Chem model and B.A.N., D.S.J,
676 and J.L.J. analyzed the model output. B.A.N., P.L.H., J.M.S., and J.L.J. ran and analyzed the 0-D
677 model used for ASOA budget analysis of ambient observations. B.C.M., A.L., M.L., and Q.Z.
678 analyzed and provided the emission inventories used for the 0-D box model. D.S.J., D.K.H., and
679 M.O.N. conducted the ASOA attribution to mortality calculation, and B.A.N., D.S.J., D.K.H.,
680 M.O.N., J.A.dG, and J.L.J analyzed the results. All authors reviewed the paper.



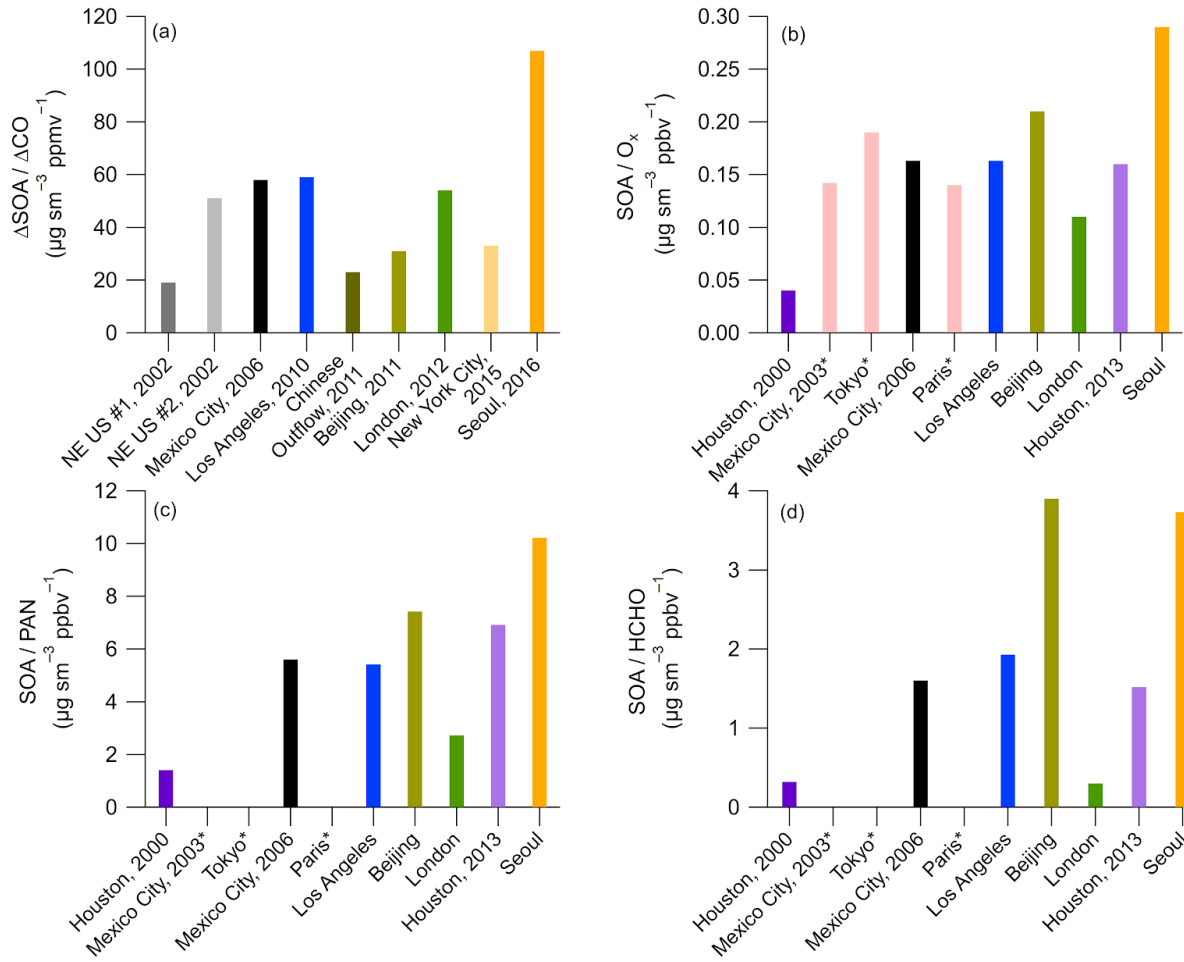


686



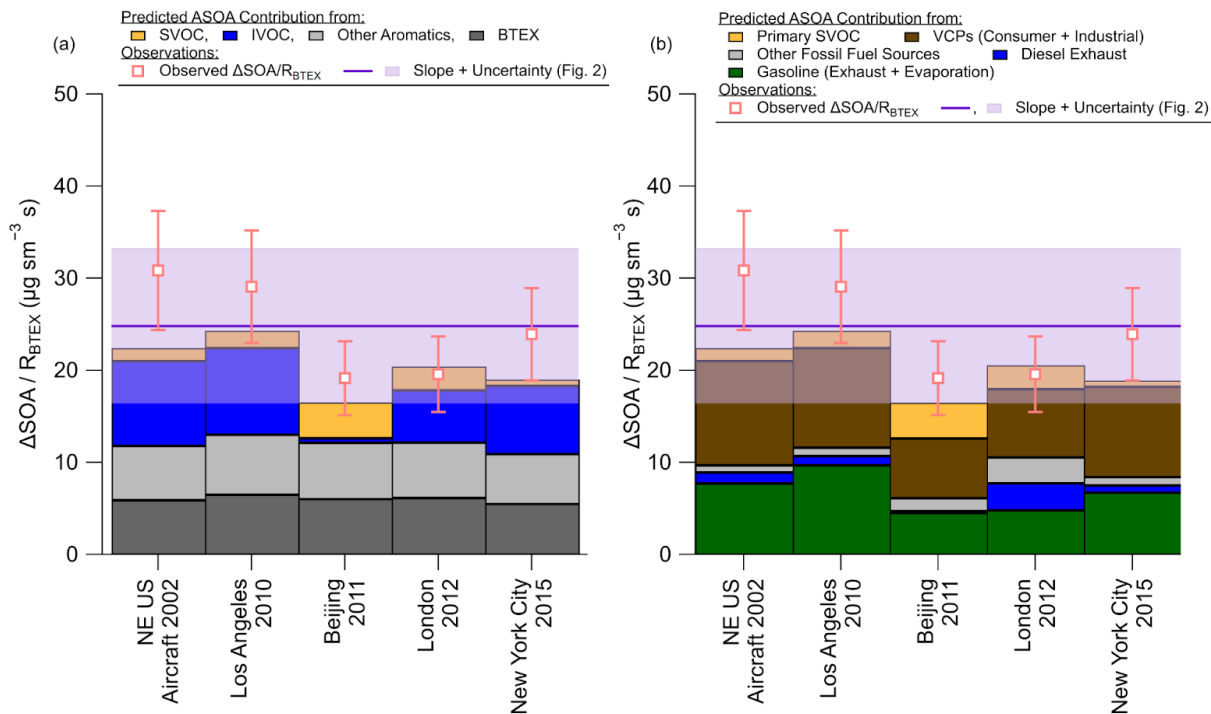
687 **Figure 2.** (a) Scatter plot of background and dilution corrected ASOA concentrations
 688 ($\Delta\text{SOA}/\Delta\text{CO}$ at PA = 0.5 equivalent days) versus BTEX emission reactivity ratio ($R_{\text{BTEX}} =$
 689 $\sum_i [\text{VOC}/\text{CO}]_i$) for multiple major field campaigns on three continents. Comparison of ASOA
 690 versus (b) O_x, (c) PAN, and (d) HCHO slopes versus the ratio of the BTEX/Total emission
 691 reactivity, where total is the OH reactivity for the emissions of BTEX + C2-3 alkenes + C2-6
 692 alkanes (Table S5 through Table S7), for the campaigns studied here. For all figures, red shading
 693 is the $\pm 1\sigma$ uncertainty of the slope, and the bars are $\pm 1\sigma$ uncertainty of the data (see Sect. S5).

694

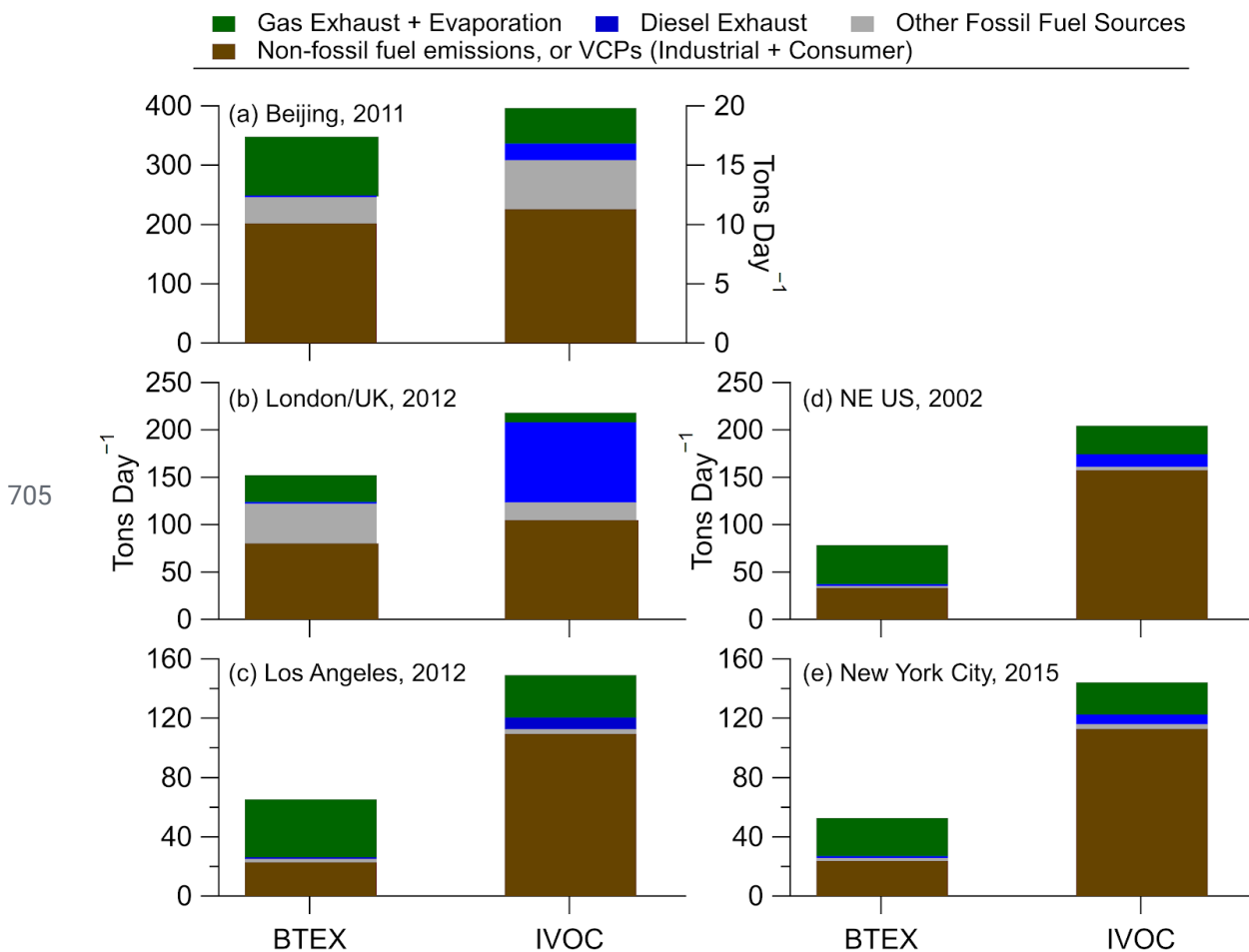


695 **Figure 3.** (a) A comparison of the $\Delta\text{SOA}/\Delta\text{CO}$ for the urban campaigns on three continents.
 696 Comparison of (b) SOA/O_x , (c) SOA/HCHO , and (d) SOA/PAN slopes for the urban areas
 697 (Table S4). For (b) through (d), cities marked with * have no HCHO, PAN, or hydrocarbon data.

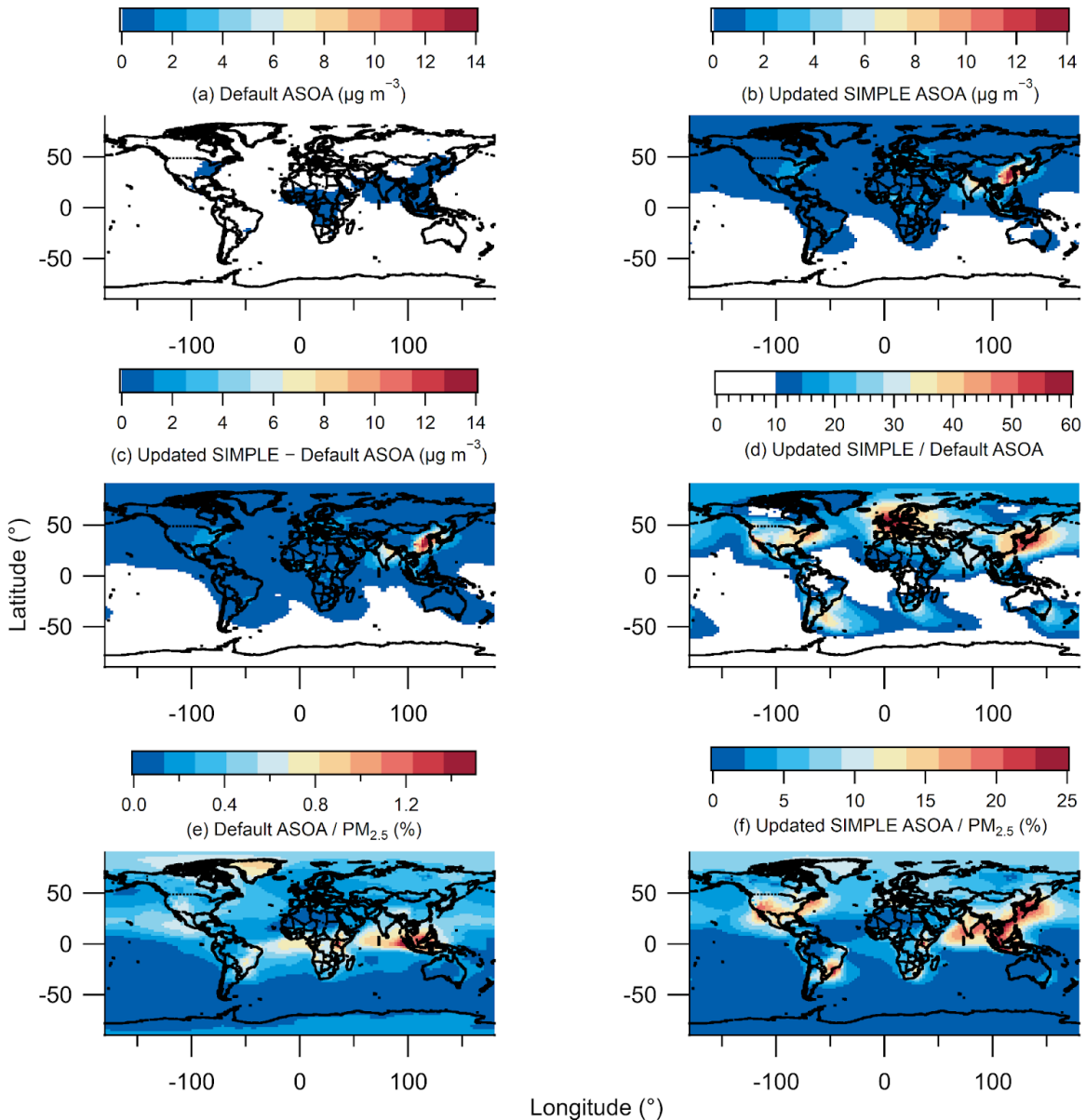
698



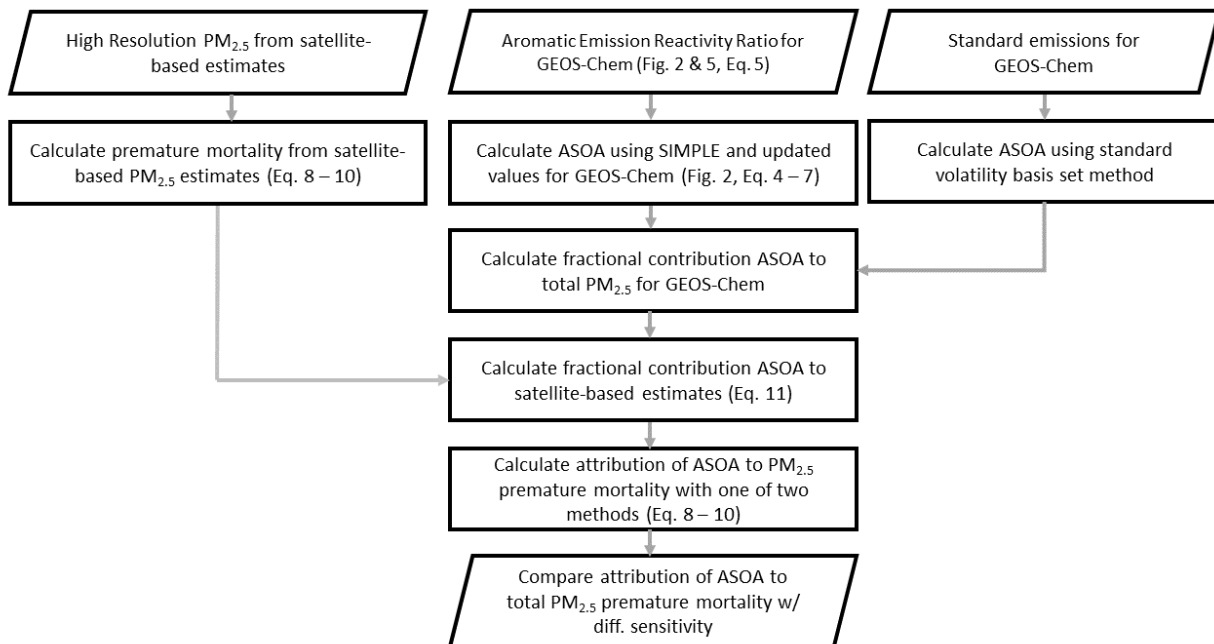
699 **Figure 4.** (a) Budget analysis for the contribution of the observed $\Delta\text{SOA}/R_{\text{BTEX}}$ (Fig. 2) for cities
 700 with known emissions inventories for different volatility classes (see SI and Fig. 5 and Fig. S6).
 701 (b) Same as (a), but for sources of emissions. For (a) and (b), SVOC is the contribution from
 702 both vehicle and other (cooking, etc.) sources. See SI for information about the emissions,
 703 ASOA precursor contribution, error analysis, and discussion about sensitivity of emission
 704 inventory IVOC/BTEX ratios for different cities and years in the US.



706 **Figure 5.** Comparison of BTEX and IVOC sources for (a) Beijing (see SI section about Beijing
 707 emission inventory), (b) London (see SI section about London/UK emission inventory), and (c)
 708 Los Angeles, (d) Northeast United States, and (e) New York City (see SI section about United
 709 States for (c) – (e)). For (a), BTEX is on the left axis and IVOC is on the right axis, due to the
 710 small emissions per day for IVOC.

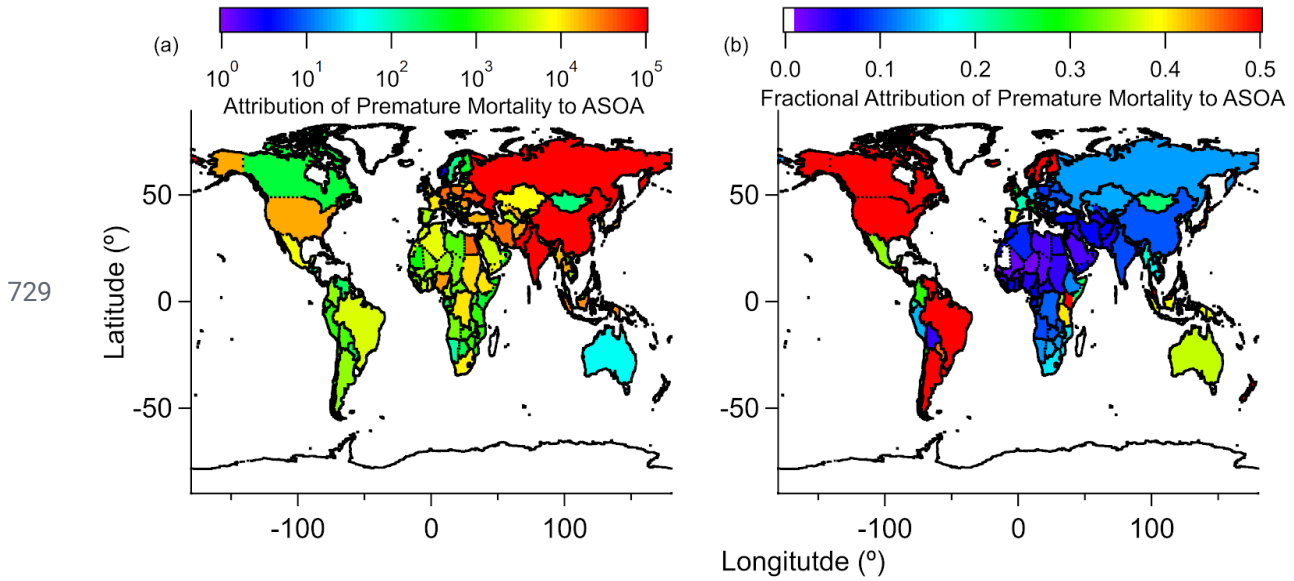


712 **Figure 6.** (a) Annual average modeled ASOA using the default VBS. (b) Annual average
 713 modeled ASOA using the updated SIMPLE model. (c) Difference between annual average
 714 modeled updated SIMPLE and default VBS. Note, for (a) - (b), values less than $0.05 \mu\text{g m}^{-3}$ are
 715 white, and for (c), values less than $0.02 \mu\text{g m}^{-3}$ are white. (d) Ratio between annual average
 716 modeled updated SIMPLE (b) and default VBS (a). (e) Percent contribution of annual average
 717 modeled ASOA using default VBS to total modelled $PM_{2.5}$. (f) Percent contribution of annual
 718 average modeled ASOA using updated SIMPLE to total modelled $PM_{2.5}$.

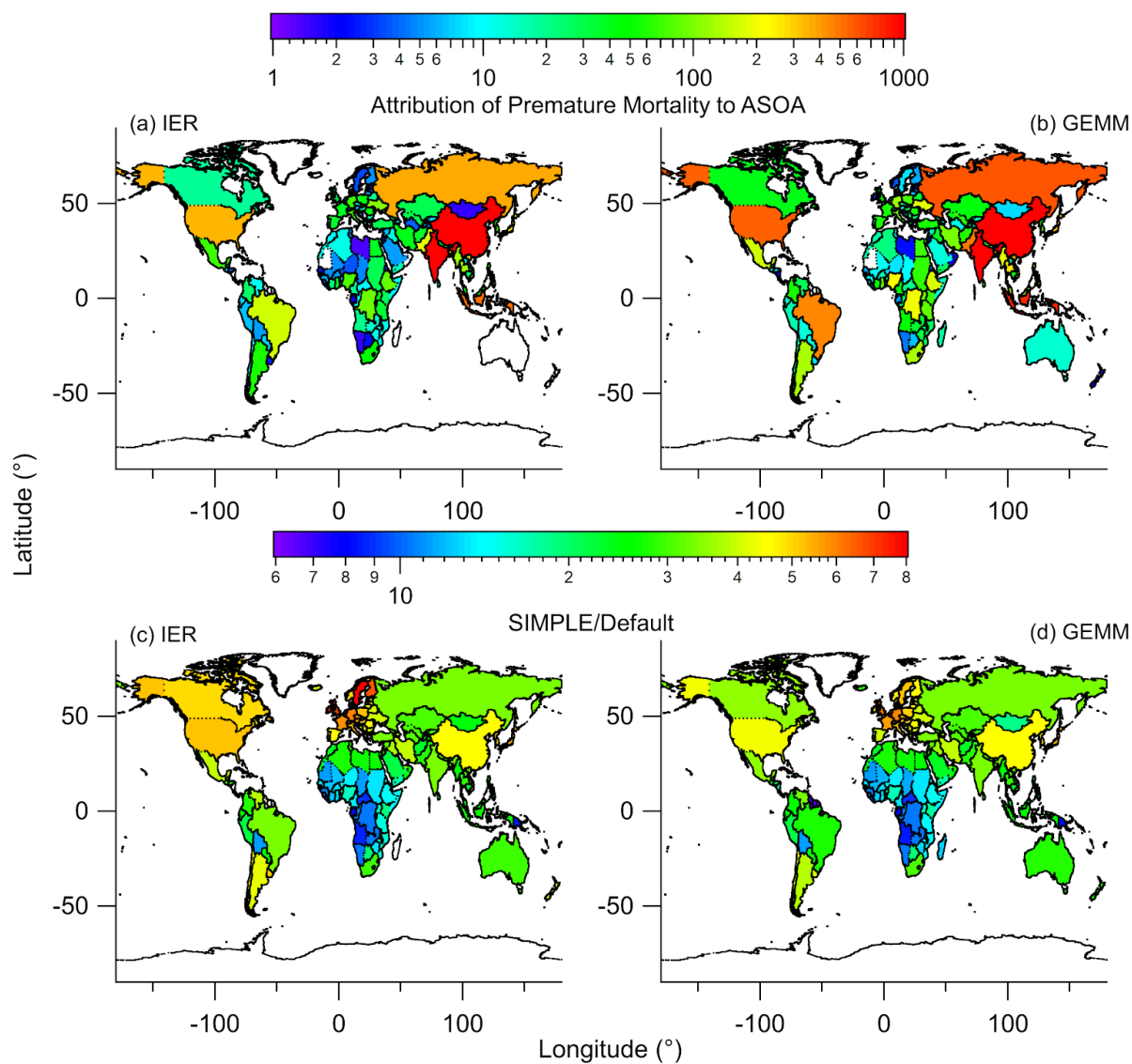


719

720 **Figure 7.** Flowchart describing how observed ASOA production was used to calculate ASOA in
 721 GEOS-Chem, and how the satellite-based PM_{2.5} estimates and GEOS-Chem PM_{2.5} speciation was
 722 used to estimate the premature mortality and attribution of premature mortality by ASOA. See
 723 Sect. 2 and SI for further information about the details in the figure. SIMPLE is described in
 724 Eq. 4 and by Hodzic and Jimenez (2011) and Hayes et al. (2015). The one of two methods
 725 mentioned include either the Integrated Exposure-Response (IER) (Burnett et al., 2014) with
 726 Global Burden of Disease (GBD) dataset (IHME, 2016) or the new Global Exposure Mortality
 727 Model (GEMM) (Burnett et al., 2018) methods. For both IER and GEMM, the marginal method
 728 (Silva et al., 2016) or attributable fraction method (Anenberg et al., 2019) are used.



730 **Figure 8.** Five-year average (a) estimated reduction in $PM_{2.5}$ -associated premature deaths, by
 731 country, upon removing ASOA from total $PM_{2.5}$, and (b) fractional reduction (reduction $PM_{2.5}$
 732 premature deaths / total $PM_{2.5}$ premature deaths) in $PM_{2.5}$ -associated premature deaths, by
 733 country, upon removing ASOA from GEOS-Chem. The IER methods are used here. See Fig. S9
 734 and Fig. S12 for results using GEMM. See Fig. S10 for 10×10 km² area results in comparison
 735 with country-level results.



736

737 **Figure 9.** Attribution of premature mortality to ASOA using (a) IER or (b) GEMM, using the
 738 non-volatile primary OA and traditional SOA precursor method in prior studies (e.g., Ridley et
 739 al., 2018). The increase in attribution of premature mortality to ASOA for the “SIMPLE” model
 740 (Fig. 8) versus the non-volatile primary OA and traditional SOA precursor method (“Default”),
 741 for (c) IER and (d) GEMM.

742 **Table 1.** List of campaigns used here. For values previously reported for those campaigns, they
 743 are noted. For Seasons, W = Winter, Sp = Spring, and Su = Summer.

Location	Field Campaign	Coordinates		Time Period	Season	Previous Publication/Campaign Overview
		Long. (°)	Lat. (°)			
Houston, TX, USA (2000)	TexAQS 2000	-95.4	29.8	15/Aug/2000 - 15/Sept/2000	Su	Jimenez et al. (2009) ^a , Wood et al. (2010) ^b
Northeast USA (2002)	NEAQS 2002	-78.1 - -70.5	32.8 - 43.1	26/July/2002; 29/July/2002 - 10/Aug/2002	Su	Jimenez et al. (2009) ^a , de Gouw and Jimenez (2009) ^c , Kleinman et al. (2007) ^c
Mexico City, Mexico (2003)	MCMA-2003	-99.2	19.5	31/Mar/2003 - 04/May/2003	Sp	Molina et al. (2007), Herndon et al. (2008) ^b
Tokyo, Japan (2004)		139.7	35.7	24/July/2004 - 14/Aug/2004	Su	Kondo et al. (2008) ^a , Miyakawa et al. (2008) ^a , Morino et al. (2014) ^b
Mexico City, Mexico (2006)	MILAGRO	-99.4 - -98.6	19.0 - 19.8	04/Mar/2006 - 29/Mar/2006	Sp	Molina et al. (2010), DeCarlo et al. (2008) ^a , Wood et al. (2010) ^b , DeCarlo et al. (2010) ^c
Paris, France (2009)	MEGAPOLI	48.9	2.4	13/July/2009 - 29/July/2009	Su	Frenay et al. (2014) ^a , Zhang et al. (2015) ^b
Pasadena, CA, USA (2010)	CalNex	-118.1	34.1	15/May/2010 - 16/June/2010	Sp	Ryerson et al. (2013), Hayes et al. (2013) ^{a,b,c}
Changdao Island, China (2011)	CAPTAIN	120.7	38.0	21/Mar/2011 - 24/Apr/2011	Sp	Hu et al. (2013) ^{a,c}
Beijing, China (2011)	CareBeijing 2011	116.4	39.9	03/Aug/2011 - 15/Sept/2011	Su	Hu et al. (2016) ^{a,b,c}
London, UK (2012)	ClearfLo	0.1	51.5	22/July/2012 - 18/Aug/2012	Su	Bohnenstengel et al. (2015)
Houston, TX, USA (2013)	SEAC ⁴ RS	-96.0 - -94.0	29.2 - 30.3	01/Aug/2013 - 23/Sept/2013	Su	Toon et al. (2016)
New York City, NY, USA (2015)	WINTER	-74.0 - -69.0	39.5 - 42.5	07/Feb/2015	W	Schroder et al. (2018) ^{a,c}
Seoul, South Korea (2016)	KORUS-AQ	124.6 - 128.0	36.8 - 37.6	01/May/2016 - 10/June/2016	Sp	Nault et al. (2018) ^{a,b,c,d}

744 ^aReference used for PM₁ composition. ^bReference used for SOA/O_x slope. ^cReference used for
 745 ΔOA/ΔCO value. ^dReference used for SOA/HCHO and SOA/PAN slopes

746 References

- 747 Anenberg, S., Miller, J., Henze, D. and Minjares, R.: A global snapshot of the air
748 pollution-related health impacts of transportation sector emissions in 2010 and 2015, ICCT,
749 Climate & Clean Air Coalition., 2019.
- 750 Atkinson, R. and Arey, J.: Atmospheric Degradation of Volatile Organic Compounds, Chem.
751 Rev., 103, 4605–4638, 2003.
- 752 Atkinson, R., Baulch, D. L., Cox, R. A., Crowley, J. N., Hampson, R. F., Hynes, R. G., Jenkin,
753 M. E., Rossi, M. J., Troe, J. and IUPAC Subcommittee: Evaluated kinetic and photochemical
754 data for atmospheric chemistry: Volume II - gas phase reactions of organic species, Atmos.
755 Chem. Phys., 6(11), 3625–4055, 2006.
- 756 Bae, M.-S., Demerjian, K. L. and Schwab, J. J.: Seasonal estimation of organic mass to organic
757 carbon in PM_{2.5} at rural and urban locations in New York state, Atmos. Environ., 40(39),
758 7467–7479, 2006.
- 759 Baker, K. R., Woody, M. C., Valin, L., Szykman, J., Yates, E. L., Iraci, L. T., Choi, H. D., Soja,
760 A. J., Koplitz, S. N., Zhou, L., Campuzano-Jost, P., Jimenez, J. L. and Hair, J. W.: Photochemical
761 model evaluation of 2013 California wild fire air quality impacts using surface, aircraft, and
762 satellite data, Sci. Total Environ., 637-638, 1137–1149, 2018.
- 763 Bertram, T. H., Perring, A. E., Wooldridge, P. J., Crouse, J. D., Kwan, A. J., Wennberg, P. O.,
764 Scheuer, E., Dibb, J., Avery, M., Sachse, G., Vay, S. A., Crawford, J. H., McNaughton, C. S.,
765 Clarke, A., Pickering, K. E., Fuelberg, H., Huey, G., Blake, D. R., Singh, H. B., Hall, S. R.,
766 Shetter, R. E., Fried, A., Heikes, B. G. and Cohen, R. C.: Direct Measurements of the Convective
767 Recycling of the Upper Troposphere, Science, 315(5813), 816–820, 2007.
- 768 Bohnenstengel, S. I., Belcher, S. E., Aiken, A., Allan, J. D., Allen, G., Bacak, A., Bannan, T. J.,
769 Barlow, J. F., Beddows, D. C. S., Bloss, W. J., Booth, A. M., Chemel, C., Coceal, O., Di Marco,
770 C. F., Dubey, M. K., Faloon, K. H., Fleming, Z. L., Furger, M., Gietl, J. K., Graves, R. R., Green,
771 D. C., Grimmond, C. S. B., Halios, C. H., Hamilton, J. F., Harrison, R. M., Heal, M. R., Heard,
772 D. E., Helfter, C., Herndon, S. C., Holmes, R. E., Hopkins, J. R., Jones, A. M., Kelly, F. J.,
773 Kotthaus, S., Langford, B., Lee, J. D., Leigh, R. J., Lewis, A. C., Lidster, R. T., Lopez-Hilfiker,
774 F. D., McQuaid, J. B., Mohr, C., Monks, P. S., Nemitz, E., Ng, N. L., Percival, C. J., Prévôt, A. S.
775 H., Ricketts, H. M. A., Sokhi, R., Stone, D., Thornton, J. A., Tremper, A. H., Valach, A. C.,
776 Visser, S., Whalley, L. K., Williams, L. R., Xu, L., Young, D. E., Zotter, P., Bohnenstengel, S. I.,
777 Belcher, S. E., Aiken, A., Allan, J. D., Allen, G., Bacak, A., Bannan, T. J., Barlow, J. F.,
778 Beddows, D. C. S., Bloss, W. J., Booth, A. M., Chemel, C., Coceal, O., Marco, C. F. D., Dubey,
779 M. K., Faloon, K. H., Fleming, Z. L., Furger, M., Gietl, J. K., Graves, R. R., Green, D. C.,
780 Grimmond, C. S. B., Halios, C. H., Hamilton, J. F., Harrison, R. M., Heal, M. R., Heard, D. E.,
781 Helfter, C., Herndon, S. C., Holmes, R. E., Hopkins, J. R., Jones, A. M., Kelly, F. J., Kotthaus,
782 S., Langford, B., Lee, J. D., Leigh, R. J., Lewis, A. C., Lidster, R. T., Lopez-Hilfiker, F. D., et al.:
783 Meteorology, Air Quality, and Health in London: The ClearfLo Project, Bull. Am. Meteorol.

784 Soc., 96(5), 779–804, 2015.

785 Burnett, R., Chen, H., Szyszkowicz, M., Fann, N., Hubbell, B., Pope, C. A., Apte, J. S., Brauer,
786 M., Cohen, A., Weichenthal, S., Coggins, J., Di, Q., Brunekreef, B., Frostad, J., Lim, S. S., Kan,
787 H., Walker, K. D., Thurston, G. D., Hayes, R. B., Lim, C. C., Turner, M. C., Jerrett, M., Krewski,
788 D., Gapstur, S. M., Diver, W. R., Ostro, B., Goldberg, D., Crouse, D. L., Martin, R. V., Peters, P.,
789 Pinault, L., Tjepkema, M., van Donkelaar, A., Villeneuve, P. J., Miller, A. B., Yin, P., Zhou, M.,
790 Wang, L., Janssen, N. A. H., Marra, M., Atkinson, R. W., Tsang, H., Quoc Thach, T., Cannon, J.
791 B., Allen, R. T., Hart, J. E., Laden, F., Cesaroni, G., Forastiere, F., Weinmayr, G., Jaensch, A.,
792 Nagel, G., Concin, H. and Spadaro, J. V.: Global estimates of mortality associated with long-term
793 exposure to outdoor fine particulate matter, *Proc. Natl. Acad. Sci. U. S. A.*, 115(38), 9592–9597,
794 2018.

795 Burnett, R. T., Pope, C. A., Ezzati, M., Olives, C., Lim, S. S., Mehta, S., Shin, H. H., Singh, G.,
796 Hubbell, B., Brauer, M., Anderson, H. R., Smith, K. R., Balmes, J. R., Bruce, N. G., Kan, H.,
797 Laden, F., Prüss-Ustün, A., Turner, M. C., Gapstur, S. M., Diver, W. R. and Cohen, A.: An
798 integrated risk function for estimating the global burden of disease attributable to ambient fine
799 particulate matter exposure, *Environ. Health Perspect.*, 122(4), 397–403, 2014.

800 Cappa, C. D., Jathar, S. H., Kleeman, M. J., Docherty, K. S., Jimenez, J. L., Seinfeld, J. H. and
801 Wexler, A. S.: Simulating secondary organic aerosol in a regional air quality model using the
802 statistical oxidation model - Part 2: Assessing the influence of vapor wall losses, *Atmos. Chem.*
803 *Phys.*, 16(5), 3041–3059, 2016.

804 Chafe, Z., Brauer, M., Heroux, M.-E., Klimont, Z., Lanki, T., Salonen, R. O. and Smith, K. R.:
805 Residential heating with wood and coal: Health impacts and policy options in Europe and North
806 America, WHO/UNECE LRTAP., 2015.

807 CIESIN: Gridded Population of the World (GPW), v4, SEDAC [online] Available from:
808 <https://sedac.ciesin.columbia.edu/data/collection/gpw-v4> (Accessed 12 May 2020), 2017.

809 Coggon, M. M., McDonald, B. C., Vlasenko, A., Veres, P. R., Bernard, F., Koss, A. R., Yuan, B.,
810 Gilman, J. B., Peischl, J., Aikin, K. C., DuRant, J., Warneke, C., Li, S.-M. and de Gouw, J. A.:
811 Diurnal Variability and Emission Pattern of Decamethylcyclopentasiloxane (D₅) from the
812 Application of Personal Care Products in Two North American Cities, *Environ. Sci. Technol.*,
813 52(10), 5610–5618, 2018.

814 Cohen, A. J., Brauer, M., Burnett, R., Anderson, H. R., Frostad, J., Estep, K., Balakrishnan, K.,
815 Brunekreef, B., Dandona, L., Dandona, R., Feigin, V., Freedman, G., Hubbell, B., Jobling, A.,
816 Kan, H., Knibbs, L., Liu, Y., Martin, R., Morawska, L., Pope, C. A., Shin, H., Straif, K.,
817 Shaddick, G., Thomas, M., van Dingenen, R., van Donkelaar, A., Vos, T., Murray, C. J. L. and
818 Forouzanfar, M. H.: Estimates and 25-year trends of the global burden of disease attributable to
819 ambient air pollution: an analysis of data from the Global Burden of Diseases Study 2015,
820 *Lancet*, 389(10082), 1907–1918, 2017.

821 DeCarlo, P. F., Dunlea, E. J., Kimmel, J. R., Aiken, A. C., Sueper, D., Crounse, J., Wennberg, P.

822 O., Emmons, L., Shinozuka, Y., Clarke, A., Zhou, J., Tomlinson, J., Collins, D. R., Knapp, D.,
823 Weinheimer, A. J., Montzka, D. D., Campos, T. and Jimenez, J. L.: Fast airborne aerosol size and
824 chemistry measurements above Mexico City and Central Mexico during the MILAGRO
825 campaign, *Atmos. Chem. Phys.*, 8(14), 4027–4048, 2008.

826 DeCarlo, P. F., Ulbrich, I. M., Crouse, J., de Foy, B., Dunlea, E. J., Aiken, A. C., Knapp, D.,
827 Weinheimer, A. J., Campos, T., Wennberg, P. O. and Jimenez, J. L.: Investigation of the sources
828 and processing of organic aerosol over the Central Mexican Plateau from aircraft measurements
829 during MILAGRO, *Atmos. Chem. Phys.*, 10(12), 5257–5280, 2010.

830 Deming, B., Pagonis, D., Liu, X., Talukdar, R. K., Roberts, J. M., Veres, P. R., Krechmer, J. E.,
831 de Gouw, J. A., Jimenez, J. L. and Ziemann, P. J.: Measurements of Delays of Gas-Phase
832 Compounds in a Wide Variety of Tubing Materials due to Gas-Wall Partitioning, *Atmos. Meas.*
833 *Tech.*, In Prep., 2018.

834 Dominutti, P., Keita, S., Bahino, J., Colomb, A., Lioussé, C., Yoboué, V., Galy-Lacaux, C.,
835 Morris, E., Bouvier, L., Sauvage, S. and Borbon, A.: Anthropogenic VOCs in Abidjan, southern
836 West Africa: from source quantification to atmospheric impacts, *Atmos. Chem. Phys.*, 19(18),
837 11721–11741, 2019.

838 van Donkelaar, A., Martin, R. V., Brauer, M. and Boys, B. L.: Use of Satellite Observations for
839 Long-Term Exposure Assessment of Global Concentrations of Fine Particulate Matter, *Environ.*
840 *Health Perspect.*, 123(2), 135–143, 2015.

841 van Donkelaar, A., Martin, R. V., Brauer, M., Hsu, N. C., Kahn, R. A., Levy, R. C., Lyapustin,
842 A., Sayer, A. M. and Winker, D. M.: Global Estimates of Fine Particulate Matter using a
843 Combined Geophysical-Statistical Method with Information from Satellites, Models, and
844 Monitors, *Environ. Sci. Technol.*, 50(7), 3762–3772, 2016.

845 Dzepina, K., Volkamer, R. M., Madronich, S., Tulet, P., Ulbrich, I. M., Zhang, Q., Cappa, C. D.,
846 Ziemann, P. J. and Jimenez, J. L.: Evaluation of recently-proposed secondary organic aerosol
847 models for a case study in Mexico City, *Atmos. Chem. Phys.*, 9(15), 5681–5709, 2009.

848 EMEP/EEA: EMEP/EEA Air Pollutant Emission Inventory Guidebook 2016, EEA,
849 Luxembourg., 2016.

850 Ensberg, J. J., Hayes, P. L., Jimenez, J. L., Gilman, J. B., Kuster, W. C., de Gouw, J. A.,
851 Holloway, J. S., Gordon, T. D., Jathar, S., Robinson, A. L. and Seinfeld, J. H.: Emission factor
852 ratios, SOA mass yields, and the impact of vehicular emissions on SOA formation, *Atmos.*
853 *Chem. Phys.*, 14(5), 2383–2397, 2014.

854 Freney, E. J., Sellegri, K., Canonaco, F., Colomb, A., Borbon, A., Michoud, V., Crumeyrolle, S.,
855 Amarouche, N., Bourianne, T., Gomes, L., Prevot, A. S. H., Beekmann, M. and
856 Schwarzenböeck, A.: Characterizing the impact of urban emissions on regional aerosol particles:
857 Airborne measurements during the MEGAPOLI experiment, *Atmos. Chem. Phys.*, 14(3),
858 1397–1412, 2014.

859 Gentner, D. R., Isaacman, G., Worton, D. R., Chan, A. W. H., Dallmann, T. R., Davis, L., Liu, S.,
860 Day, D. A., Russell, L. M., Wilson, K. R., Weber, R., Guha, A., Harley, R. A. and Goldstein, A.
861 H.: Elucidating secondary organic aerosol from diesel and gasoline vehicles through detailed
862 characterization of organic carbon emissions, *Proc. Natl. Acad. Sci. U. S. A.*, 109(45),
863 18318–18323, 2012.

864 Goel, R. and Guttikunda, S. K.: Evolution of on-road vehicle exhaust emissions in Delhi, *Atmos.*
865 *Environ.*, 105, 78–90, 2015.

866 de Gouw, J. A. and Jimenez, J. L.: Organic Aerosols in the Earth's Atmosphere, *Environ. Sci.*
867 *Technol.*, 43(20), 7614–7618, 2009.

868 de Gouw, J. A., Middlebrook, A. M., Warneke, C., Goldan, P. D., Kuster, W. C., Roberts, J. M.,
869 Fehsenfeld, F. C., Worsnop, D. R., Canagaratna, M. R., Pszenny, A. A. P., Keene, W. C.,
870 Marchewka, M., Bertman, S. B. and Bates, T. S.: Budget of organic carbon in a polluted
871 atmosphere: Results from the New England Air Quality Study in 2002, *J. Geophys. Res. D:*
872 *Atmos.*, 110(16), 1–22, 2005.

873 de Gouw, J. A., Gilman, J. B., Kim, S.-W., Lerner, B. M., Isaacman-VanWertz, G., McDonald, B.
874 C., Warneke, C., Kuster, W. C., Lefer, B. L., Griffith, S. M., Dusanter, S., Stevens, P. S. and
875 Stutz, J.: Chemistry of Volatile Organic Compounds in the Los Angeles basin: Nighttime
876 Removal of Alkenes and Determination of Emission Ratios, *J. Geophys. Res.: Atmos.*, 122(21),
877 11,843–11,861, 2017.

878 de Gouw, J. A., Gilman, J. B., Kim, S.-W., Alvarez, S. L., Dusanter, S., Graus, M., Griffith, S.
879 M., Isaacman-VanWertz, G., Kuster, W. C., Lefer, B. L., Lerner, B. M., McDonald, B. C.,
880 Rappenglück, B., Roberts, J. M., Stevens, P. S., Stutz, J., Thalman, R., Veres, P. R., Volkamer, R.,
881 Warneke, C., Washenfelder, R. A. and Young, C. J.: Chemistry of volatile organic compounds in
882 the Los Angeles basin: Formation of oxygenated compounds and determination of emission
883 ratios, *J. Geophys. Res.*, 123(4), 2298–2319, 2018.

884 Grieshop, A. P., Logue, J. M., Donahue, N. M. and Robinson, A. L.: Laboratory investigation of
885 photochemical oxidation of organic aerosol from wood fires 1: measurement and simulation of
886 organic aerosol evolution, *Atmos. Chem. Phys.*, 9(4), 1263–1277, 2009.

887 Hallquist, M., Wenger, J. C., Baltensperger, U., Rudich, Y., Simpson, D., Claeys, M., Dommen,
888 J., Donahue, N. M., George, C., Goldstein, A. H., Hamilton, J. F., Herrmann, H., Hoffmann, T.,
889 Iinuma, Y., Jang, M., Jenkin, M. E., Jimenez, J. L., Kiendler-Scharr, A., Maenhaut, W.,
890 McFiggans, G., Mentel, T. F., Monod, A., Prévôt, A. S. H., Seinfeld, J. H., Surratt, J. D.,
891 Szmigielski, R. and Wildt, J.: The formation, properties and impact of secondary organic aerosol:
892 current and emerging issues, *Atmos. Chem. Phys.*, 9(14), 5155–5236, 2009.

893 Hayes, P. L., Ortega, A. M., Cubison, M. J., Froyd, K. D., Zhao, Y., Cliff, S. S., Hu, W. W.,
894 Toohey, D. W., Flynn, J. H., Lefer, B. L., Grossberg, N., Alvarez, S., Rappenglück, B., Taylor, J.
895 W., Allan, J. D., Holloway, J. S., Gilman, J. B., Kuster, W. C., de Gouw, J. A., Massoli, P.,
896 Zhang, X., Liu, J., Weber, R. J., Corrigan, A. L., Russell, L. M., Isaacman, G., Worton, D. R.,

897 Kreisberg, N. M., Goldstein, A. H., Thalman, R., Waxman, E. M., Volkamer, R., Lin, Y. H.,
898 Surratt, J. D., Kleindienst, T. E., Offenberg, J. H., Dusanter, S., Griffith, S., Stevens, P. S.,
899 Brioude, J., Angevine, W. M. and Jimenez, J. L.: Organic aerosol composition and sources in
900 Pasadena, California, during the 2010 CalNex campaign, *J. Geophys. Res. D: Atmos.*, 118(16),
901 9233–9257, 2013.

902 Hayes, P. L., Carlton, A. G., Baker, K. R., Ahmadov, R., Washenfelder, R. A., Alvarez, S.,
903 Rappenglück, B., Gilman, J. B., Kuster, W. C., de Gouw, J. A., Zotter, P., Prévôt, A. S. H.,
904 Szidat, S., Kleindienst, T. E., Ma, P. K. and Jimenez, J. L.: Modeling the formation and aging of
905 secondary organic aerosols in Los Angeles during CalNex 2010, *Atmos. Chem. Phys.*, 15(10),
906 5773–5801, 2015.

907 Heringa, M. F., DeCarlo, P. F., Chirico, R., Tritscher, T., Dommen, J., Weingartner, E., Richter,
908 R., Wehrle, G., Prévôt, A. S. H. and Baltensperger, U.: Investigations of primary and secondary
909 particulate matter of different wood combustion appliances with a high-resolution time-of-flight
910 aerosol mass spectrometer, *Atmos. Chem. Phys.*, 11(12), 5945–5957, 2011.

911 Herndon, S. C., Onasch, T. B., Wood, E. C., Kroll, J. H., Canagaratna, M. R., Jayne, J. T.,
912 Zavala, M. A., Knighton, W. B., Mazzoleni, C., Dubey, M. K., Ulbrich, I. M., Jimenez, J. L.,
913 Seila, R., de Gouw, J. A., de Foy, B., Fast, J., Molina, L. T., Kolb, C. E. and Worsnop, D. R.:
914 Correlation of secondary organic aerosol with odd oxygen in Mexico City, *Geophys. Res. Lett.*,
915 35(15), L15804, 2008.

916 Hodzic, A. and Jimenez, J. L.: Modeling anthropogenically controlled secondary organic
917 aerosols in a megacity: A simplified framework for global and climate models, *Geosci. Model*
918 *Dev.*, 4(4), 901–917, 2011.

919 Hodzic, A., Jimenez, J. L., Madronich, S., Aiken, A. C., Bessagnet, B., Curci, G., Fast, J.,
920 Lamarque, J.-F., Onasch, T. B., Roux, G., Schauer, J. J., Stone, E. A. and Ulbrich, I. M.:
921 Modeling organic aerosols during MILAGRO: importance of biogenic secondary organic
922 aerosols, *Atmos. Chem. Phys.*, 9(18), 6949–6981, 2009.

923 Hodzic, A., Jimenez, J. L., Prévôt, A. S. H., Szidat, S., Fast, J. D. and Madronich, S.: Can 3-D
924 models explain the observed fractions of fossil and non-fossil carbon in and near Mexico City?,
925 *Atmos. Chem. Phys.*, 10(22), 10997–11016, 2010a.

926 Hodzic, A., Jimenez, J. L., Madronich, S., Canagaratna, M. R., DeCarlo, P. F., Kleinman, L. and
927 Fast, J.: Modeling organic aerosols in a megacity: potential contribution of semi-volatile and
928 intermediate volatility primary organic compounds to secondary organic aerosol formation,
929 *Atmos. Chem. Phys.*, 10(12), 5491–5514, 2010b.

930 Hodzic, A., Campuzano-Jost, P., Bian, H., Chin, M., Colarco, P. R., Day, D. A., Froyd, K. D.,
931 Heinold, B., Jo, D. S., Katich, J. M., Kodros, J. K., Nault, B. A., Pierce, J. R., Ray, E., Schacht,
932 J., Schill, G. P., Schroder, J. C., Schwarz, J. P., Sueper, D. T., Tegen, I., Tilmes, S., Tsigaridis, K.,
933 Yu, P. and Jimenez, J. L.: Characterization of Organic Aerosol across the Global Remote
934 Troposphere: A comparison of ATOM measurements and global chemistry models, *Atmos.*

935 Chem. Phys., 20(8), 4607–4635, 2020.

936 Hu, W., Hu, M., Hu, W., Jimenez, J. L., Yuan, B., Chen, W., Wang, M., Wu, Y., Chen, C., Wang,
937 Z., Peng, J., Zeng, L. and Shao, M.: Chemical composition, sources, and aging process of
938 submicron aerosols in Beijing: Contrast between summer and winter, J. Geophys. Res. D:
939 Atmos., 121(4), 1955–1977, 2016.

940 Hu, W., Downward, G., Wong, J. Y. Y., Reiss, B., Rothman, N., Portengen, L., Li, J., Jones, R.
941 R., Huang, Y., Yang, K., Chen, Y., Xu, J., He, J., Bassig, B., Seow, W. J., Hosgood, H. D., Zhang,
942 L., Wu, G., Wei, F., Vermeulen, R. and Lan, Q.: Characterization of outdoor air pollution from
943 solid fuel combustion in Xuanwei and Fuyuan, a rural region of China, Sci. Rep., 10(1), 11335,
944 2020.

945 Hu, W. W., Hu, M., Yuan, B., Jimenez, J. L., Tang, Q., Peng, J. F., Hu, W., Shao, M., Wang, M.,
946 Zeng, L. M., Wu, Y. S., Gong, Z. H., Huang, X. F. and He, L. Y.: Insights on organic aerosol
947 aging and the influence of coal combustion at a regional receptor site of central eastern China,
948 Atmos. Chem. Phys., 13(19), 10095–10112, 2013.

949 IHME: Global Burden of Disease Study 2015 (GBD 2015) Data Resources, GHDx [online]
950 Available from: <http://ghdx.healthdata.org/gbd-2015> (Accessed 2019), 2016.

951 Janssen, R. H. H., Tsimpidi, A. P., Karydis, V. A., Pozzer, A., Lelieveld, J., Crippa, M., Prévôt,
952 A. S. H., Ait-Helal, W., Borbon, A., Sauvage, S. and Locoge, N.: Influence of local production
953 and vertical transport on the organic aerosol budget over Paris, J. Geophys. Res. D: Atmos.,
954 122(15), 8276–8296, 2017.

955 Janssens-Maenhout, G., Crippa, M., Guizzardi, D., Dentener, F., Muntean, M., Pouliot, G.,
956 Keating, T., Zhang, Q., Kurokawa, J., Wankmüller, R., Denier van der Gon, H., Kuenen, J. J. P.,
957 Klimont, Z., Frost, G., Darras, S., Koffi, B. and Li, M.: HTAP_v2.2: a mosaic of regional and
958 global emission grid maps for 2008 and 2010 to study hemispheric transport of air pollution,
959 Atmos. Chem. Phys., 15(19), 11411–11432, 2015.

960 Jathar, S. H., Woody, M., Pye, H. O. T., Baker, K. R. and Robinson, A. L.: Chemical transport
961 model simulations of organic aerosol in southern California: model evaluation and gasoline and
962 diesel source contributions, Atmos. Chem. Phys., 17(6), 4305–4318, 2017.

963 Jena, C., Ghude, S. D., Kulkarni, R., Debnath, S., Kumar, R., Soni, V. K., Acharja, P., Kulkarni,
964 S. H., Khare, M., Kaginalkar, A. J., Chate, D. M., Ali, K., Nanjundiah, R. S. and Rajeevan, M.
965 N.: Evaluating the sensitivity of fine particulate matter (PM_{2.5}) simulations to chemical
966 mechanism in Delhi, Atmos. Chem. Phys. Discuss., doi:10.5194/acp-2020-673, 2020.

967 Jimenez, J. L., Canagaratna, M. R., Donahue, N. M., Prevot, A. S. H., Zhang, Q., Kroll, J. H.,
968 DeCarlo, P. F., Allan, J. D., Coe, H., Ng, N. L., Aiken, A. C., Docherty, K. S., Ulbrich, I. M.,
969 Grieshop, A. P., Robinson, A. L., Duplissy, J., Smith, J. D., Wilson, K. R., Lanz, V. A., Hueglin,
970 C., Sun, Y. L., Tian, J., Laaksonen, A., Raatikainen, T., Rautiainen, J., Vaattovaara, P., Ehn, M.,
971 Kulmala, M., Tomlinson, J. M., Collins, D. R., Cubison, M. J., Dunlea, E. J., Huffman, J. A.,

972 Onasch, T. B., Alfarra, M. R., Williams, P. I., Bower, K., Kondo, Y., Schneider, J., Drewnick, F.,
973 Borrmann, S., Weimer, S., Demerjian, K., Salcedo, D., Cottrell, L., Griffin, R., Takami, A.,
974 Miyoshi, T., Hatakeyama, S., Shimono, A., Sun, J. Y., Zhang, Y. M., Dzepina, K., Kimmel, J. R.,
975 Sueper, D., Jayne, J. T., Herndon, S. C., Trimborn, A. M., Williams, L. R., Wood, E. C.,
976 Middlebrook, A. M., Kolb, C. E., Baltensperger, U. and Worsnop, D. R.: Evolution of organic
977 aerosols in the atmosphere, *Science*, 326(5959), 1525–1529, 2009.

978 Khare, P. and Gentner, D. R.: Considering the future of anthropogenic gas-phase organic
979 compound emissions and the increasing influence of non-combustion sources on urban air
980 quality, *Atmos. Chem. Phys.*, 18(8), 5391–5413, 2018.

981 Khare, P., Machesky, J., Soto, R., He, M., Presto, A. A. and Gentner, D. R.: Asphalt-related
982 emissions are a major missing nontraditional source of secondary organic aerosol precursors, *Sci*
983 *Adv*, 6(36), doi:10.1126/sciadv.abb9785, 2020.

984 Kleinman, L. I., Daum, P. H., Lee, Y.-N., Senum, G. I., Springston, S. R., Wang, J., Berkowitz,
985 C., Hubbe, J., Zaveri, R. A., Brechtel, F. J., Jayne, J., Onasch, T. B. and Worsnop, D.: Aircraft
986 observations of aerosol composition and ageing in New England and Mid-Atlantic States during
987 the summer 2002 New England Air Quality Study field campaign, *J. Geophys. Res. D: Atmos.*,
988 112(D9), D09310, 2007.

989 Kodros, J. K., Carter, E., Brauer, M., Volckens, J., Bilsback, K. R., L'Orange, C., Johnson, M.
990 and Pierce, J. R.: Quantifying the Contribution to Uncertainty in Mortality Attributed to
991 Household, Ambient, and Joint Exposure to PM_{2.5} From Residential Solid Fuel Use, *Geohealth*,
992 2(1), 25–39, 2018.

993 Kodros, J. K., Papanastasiou, D. K., Paglione, M., Masiol, M., Squizzato, S., Florou, K.,
994 Skyllakou, K., Kaltsonoudis, C., Nenes, A. and Pandis, S. N.: Rapid dark aging of biomass
995 burning as an overlooked source of oxidized organic aerosol, *Proc. Natl. Acad. Sci. U. S. A.*,
996 117(52), 33028–33033, 2020.

997 Kondo, Y., Morino, Y., Fukuda, M., Kanaya, Y., Miyazaki, Y., Takegawa, N., Tanimoto, H.,
998 McKenzie, R., Johnston, P., Blake, D. R., Murayama, T. and Koike, M.: Formation and transport
999 of oxidized reactive nitrogen, ozone, and secondary organic aerosol in Tokyo, *J. Geophys. Res.*
1000 *D: Atmos.*, 113(D21), D21310, 2008.

1001 Krechmer, J. E., Pagonis, D., Ziemann, P. J. and Jimenez, J. L.: Quantification of Gas-Wall
1002 Partitioning in Teflon Environmental Chambers Using Rapid Bursts of Low-Volatility Oxidized
1003 Species Generated in Situ, *Environ. Sci. Technol.*, 50(11), 5757–5765, 2016.

1004 Krewski, D., Jerrett, M., Burnett, R. T., Ma, R., Hughes, E., Shi, Y., Turner, M. C., Arden, C.,
1005 Thurston, G., Calle, E. E., Thun, M. J., Beckerman, B., Deluca, P., Finkelstein, N., Ito, K.,
1006 Moore, D. K., Newbold, K. B., Ramsay, T., Ross, Z., Shin, H. and Tempalski, B.: Extended
1007 Follow-Up and Spatial Analysis of the American Cancer Society Study Linking Particulate Air
1008 Pollution and Mortality Number 140 May 2009 PRESS VERSION., 2009.

1009 Lacey, F. G., Henze, D. K., Lee, C. J., van Donkelaar, A. and Martin, R. V.: Transient climate
1010 and ambient health impacts due to national solid fuel cookstove emissions, *Proc. Natl. Acad. Sci.*
1011 *U. S. A.*, 114(6), 1269–1274, 2017.

1012 Lam, N. L., Upadhyay, B., Maharjan, S., Jagoe, K., Weyant, C. L., Thompson, R., Uprety, S.,
1013 Johnson, M. A. and Bond, T. C.: Seasonal fuel consumption, stoves, and end-uses in rural
1014 households of the far-western development region of Nepal, *Environ. Res. Lett.*, 12(12), 125011,
1015 2017.

1016 Landrigan, P. J., Fuller, R., Acosta, N. J. R., Adeyi, O., Arnold, R., Basu, N., Baldé, A. B.,
1017 Bertollini, R., Bose-O'Reilly, S., Boufford, J. I., Breyse, P. N., Chiles, T., Mahidol, C.,
1018 Coll-Seck, A. M., Cropper, M. L., Fobil, J., Fuster, V., Greenstone, M., Haines, A., Hanrahan, D.,
1019 Hunter, D., Khare, M., Krupnick, A., Lanphear, B., Lohani, B., Martin, K., Mathiasen, K. V.,
1020 McTeer, M. A., Murray, C. J. L., Ndahimananjara, J. D., Perera, F., Potočnik, J., Preker, A. S.,
1021 Ramesh, J., Rockström, J., Salinas, C., Samson, L. D., Sandilya, K., Sly, P. D., Smith, K. R.,
1022 Steiner, A., Stewart, R. B., Suk, W. A., van Schayck, O. C. P., Yadama, G. N., Yumkella, K. and
1023 Zhong, M.: The Lancet Commission on pollution and health, *Lancet*, 391(10119), 462–512,
1024 2018.

1025 Lelieveld, J., Evans, J. S., Fnais, M., Giannadaki, D. and Pozzer, A.: The contribution of outdoor
1026 air pollution sources to premature mortality on a global scale, *Nature*, 525(7569), 367–371, 2015.

1027 Liao, J., Hanisco, T. F., Wolfe, G. M., St. Clair, J., Jimenez, J. L., Campuzano-Jost, P., Nault, B.
1028 A., Fried, A., Marais, E. A., Gonzalez Abad, G., Chance, K., Jethva, H. T., Ryerson, T. B.,
1029 Warneke, C. and Wisthaler, A.: Towards a satellite formaldehyde – in situ hybrid estimate for
1030 organic aerosol abundance, *Atmos. Chem. Phys.*, 19(5), 2765–2785, 2019.

1031 Li, M., Zhang, Q., Zheng, B., Tong, D., Lei, Y., Liu, F., Chaopeng, H., Kang, S., Yan, L., Zhang,
1032 Y., Bo, Y., Su, H., Cheng, Y. and He, K.: Persistent growth of anthropogenic non-methane
1033 volatile organic compound (NMVOC) emissions in China during 1990-2017: drivers, speciation
1034 and ozone formation potential, *Atmos. Chem. Phys.*, 19, 8897–8913, 2019.

1035 Liu, X., Deming, B., Pagonis, D., Day, D. A., Palm, B. B., Talukdar, R., Roberts, J. M., Veres, P.
1036 R., Krechmer, J. E., Thornton, J. A., de Gouw, J. A., Ziemann, P. J. and Jimenez, J. L.: Effects of
1037 gas–wall interactions on measurements of semivolatile compounds and small polar molecules, ,
1038 doi:10.5194/amt-12-3137-2019, 2019.

1039 Lu, Q., Zhao, Y. and Robinson, A. L.: Comprehensive organic emission profiles for gasoline,
1040 diesel, and gas-turbine engines including intermediate and semi-volatile organic compound
1041 emissions, *Atmos. Chem. Phys.*, 18, 17637–17654, 2018.

1042 Ma, P. K., Zhao, Y., Robinson, A. L., Worton, D. R., Goldstein, A. H., Ortega, A. M., Jimenez, J.
1043 L., Zotter, P., Prévôt, A. S. H., Szidat, S. and Hayes, P. L.: Evaluating the impact of new
1044 observational constraints on P-S/IVOC emissions, multi-generation oxidation, and chamber wall
1045 losses on SOA modeling for Los Angeles, CA, *Atmos. Chem. Phys.*, 17(15), 9237–9259, 2017.

1046 McDonald, B. C., de Gouw, J. A., Gilman, J. B., Jathar, S. H., Akherati, A., Cappa, C. D.,
1047 Jimenez, J. L., Lee-Taylor, J., Hayes, P. L., McKeen, S. A., Cui, Y. Y., Kim, S.-W., Gentner, D.
1048 R., Isaacman-VanWertz, G., Goldstein, A. H., Harley, R. A., Frost, G. J., Roberts, J. M., Ryerson,
1049 T. B. and Trainer, M.: Volatile chemical products emerging as largest petrochemical source of
1050 urban organic emissions, *Science*, 359(6377), 760–764, 2018.

1051 Miyakawa, T., Takegawa, N. and Kondo, Y.: Photochemical evolution of submicron aerosol
1052 chemical composition in the Tokyo megacity region in summer, *J. Geophys. Res. D: Atmos.*,
1053 113(D14), D14304, 2008.

1054 Molina, L. T., Kolb, C. E., de Foy, B., Lamb, B. K., Brune, W. H., Jimenez, J. L.,
1055 Ramos-Villegas, R., Sarmiento, J., Paramo-Figueroa, V. H., Cardenas, B., Gutierrez-Avedoy, V.
1056 and Molina, M. J.: Air quality in North America's most populous city – overview of the
1057 MCMA-2003 campaign, *Atmos. Chem. Phys.*, 7(10), 2447–2473, 2007.

1058 Molina, L. T., Madronich, S., Gaffney, J. S., Apel, E., de Foy, B., Fast, J., Ferrare, R., Herndon,
1059 S., Jimenez, J. L., Lamb, B., Osornio-Vargas, A. R., Russell, P., Schauer, J. J., Stevens, P. S.,
1060 Volkamer, R. and Zavala, M.: An overview of the MILAGRO 2006 Campaign: Mexico City
1061 emissions and their transport and transformation, *Atmos. Chem. Phys.*, 10(18), 8697–8760,
1062 2010.

1063 Morino, Y., Tanabe, K., Sato, K. and Ohara, T.: Secondary organic aerosol model
1064 intercomparison based on secondary organic aerosol to odd oxygen ratio in Tokyo, *J. Geophys.*
1065 *Res.: Atmos.*, 119(23), 13,489–13,505, 2014.

1066 Murphy, B. N., Woody, M. C., Jimenez, J. L., Carlton, A. M. G., Hayes, P. L., Liu, S., Ng, N. L.,
1067 Russell, L. M., Setyan, A., Xu, L., Young, J., Zaveri, R. A., Zhang, Q. and Pye, H. O. T.:
1068 Semivolatile POA and parameterized total combustion SOA in CMAQv5.2: impacts on source
1069 strength and partitioning, *Atmos. Chem. Phys.*, 17(18), 11107–11133, 2017.

1070 Nault, B. A., Campuzano-Jost, P., Day, D. A., Schroder, J. C., Anderson, B., Beyersdorf, A. J.,
1071 Blake, D. R., Brune, W. H., Choi, Y., Corr, C. A., de Gouw, J. A., Dibb, J., DiGangi, J. P., Diskin,
1072 G. S., Fried, A., Huey, L. G., Kim, M. J., Knute, C. J., Lamb, K. D., Lee, T., Park, T., Pusede, S.
1073 E., Scheuer, E., Thornhill, K. L., Woo, J.-H. and Jimenez, J. L.: Secondary Organic Aerosol
1074 Production from Local Emissions Dominates the Organic Aerosol Budget over Seoul, South
1075 Korea, during KORUS-AQ, *Atmos. Chem. Phys.*, 18, 17769–17800, 2018.

1076 Pagonis, D., Krechmer, J. E., de Gouw, J., Jimenez, J. L. and Ziemann, P. J.: Effects of Gas-Wall
1077 Partitioning in Teflon Tubing and Instrumentation on Time-Resolved Measurements of
1078 Gas-Phase Organic Compounds, *Atmospheric Measurement Techniques Discussions*, 1–19,
1079 2017.

1080 Pai, S. J., Heald, C. L., Pierce, J. R., Farina, S. C., Marais, E. A., Jimenez, J. L.,
1081 Campuzano-Jost, P., Nault, B. A., Middlebrook, A. M., Coe, H., Shilling, J. E., Bahreini, R.,
1082 Dingle, J. H. and Vu, K.: An evaluation of global organic aerosol schemes using airborne

1083 observations, *Atmos. Chem. Phys.*, 20(5), 2637–2665, 2020.

1084 Parrish, D. D., Kuster, W. C., Shao, M., Yokouchi, Y., Kondo, Y., Goldan, P. D., de Gouw, J. A.,
1085 Koike, M. and Shirai, T.: Comparison of air pollutant emissions among mega-cities, *Atmos.*
1086 *Environ.*, 43(40), 6435–6441, 2009.

1087 Petit, J.-E., Favez, O., Sciare, J., Canonaco, F., Croteau, P., Močnik, G., Jayne, J., Worsnop, D.
1088 and Leoz-Garziandia, E.: Submicron aerosol source apportionment of wintertime pollution in
1089 Paris, France by double positive matrix factorization (PMF²) using an aerosol chemical
1090 speciation monitor (ACSM) and a multi-wavelength Aethalometer, *Atmos. Chem. Phys.*, 14(24),
1091 13773–13787, 2014.

1092 Platt, S. M., Haddad, I. E., Pieber, S. M., Huang, R.-J., Zardini, A. A., Clairotte, M.,
1093 Suarez-Bertoa, R., Barmet, P., Pfaffenberger, L., Wolf, R., Slowik, J. G., Fuller, S. J., Kalberer,
1094 M., Chirico, R., Dommen, J., Astorga, C., Zimmermann, R., Marchand, N., Hellebust, S.,
1095 Temime-Roussel, B., Baltensperger, U. and Prévôt, A. S. H.: Two-stroke scooters are a dominant
1096 source of air pollution in many cities, *Nat. Commun.*, 5(1), 3749, 2014.

1097 Pollack, I. B., Ryerson, T. B., Trainer, M., Neuman, J. A., Roberts, J. M. and Parrish, D. D.:
1098 Trends in ozone, its precursors, and related secondary oxidation products in Los Angeles,
1099 California: A synthesis of measurements from 1960 to 2010, *J. Geophys. Res. D: Atmos.*,
1100 118(11), 5893–5911, 2013.

1101 Pungler, E. M. and West, J. J.: The effect of grid resolution on estimates of the burden of ozone
1102 and fine particulate matter on premature mortality in the USA, *Air Qual. Atmos. Health*, 6(3),
1103 563–573, 2013.

1104 Ridley, D. A., Heald, C. L., Ridley, K. J. and Kroll, J. H.: Causes and consequences of
1105 decreasing atmospheric organic aerosol in the United States, *Proc. Natl. Acad. Sci. U. S. A.*,
1106 115(2), 290–295, 2018.

1107 Robinson, A. L., Donahue, N. M., Shrivastava, M. K., Weitkamp, E. A., Sage, A. M., Grieshop,
1108 A. P., Lane, T. E., Pierce, J. R. and Pandis, S. N.: Rethinking Organic Aerosols: Semivolatile
1109 Emissions and Photochemical Aging, *Science*, 315(5816), 1259–1262, 2007.

1110 Ryerson, T. B., Andrews, A. E., Angevine, W. M., Bates, T. S., Brock, C. A., Cairns, B., Cohen,
1111 R. C., Cooper, O. R., de Gouw, J. A., Fehsenfeld, F. C., Ferrare, R. A., Fischer, M. L., Flagan, R.
1112 C., Goldstein, A. H., Hair, J. W., Hardesty, R. M., Hostetler, C. A., Jimenez, J. L., Langford, A.
1113 O., McCauley, E., McKeen, S. A., Molina, L. T., Nenes, A., Oltmans, S. J., Parrish, D. D.,
1114 Pederson, J. R., Pierce, R. B., Prather, K., Quinn, P. K., Seinfeld, J. H., Senff, C. J., Sorooshian,
1115 A., Stutz, J., Surratt, J. D., Trainer, M., Volkamer, R., Williams, E. J. and Wofsy, S. C.: The 2010
1116 California Research at the Nexus of Air Quality and Climate Change (CalNex) field study, *J.*
1117 *Geophys. Res. D: Atmos.*, 118(11), 5830–5866, 2013.

1118 Sacks, J., Buckley, B., Alexis, N., Angrish, M., Beardslee, R., Benson, A., Brown, J., Buckley,
1119 B., Campen, M., Chan, E., Coffman, E., Davis, A., Dutton, S. J., Eftim, S., Gandy, J., Hemming,

1120 B. L., Hines, E., Holliday, K., Kerminen, V.-M., Kiomourtzoglou, M.-A., Kirrane, E., Kotchmar,
1121 D., Koturbash, I., Kulmala, M., Lassiter, M., Limaye, V., Ljungman, P., Long, T., Luben, T.,
1122 Malm, W., McDonald, J. F., McDow, S., Mickley, L., Mikati, I., Mulholland, J., Nichols, J.,
1123 Patel, M. M., Pinder, R., Pinto, J. P., Rappazzo, K., Richomond-Bryant, J., Rosa, M., Russell, A.,
1124 Schichtel, B., Stewart, M., Stanek, L. W., Turner, M., Van Winkle, L., Wagner, J., Weaver,
1125 Christopher, Wellenius, G., Whitsel, E., Yeckel, C., Zanobetti, A. and Zhang, M.: Integrated
1126 Science Assessment (ISA) for Particulate Matter (Final Report, Dec 2019), Environmental
1127 Protection Agency. [online] Available from:
1128 <https://cfpub.epa.gov/ncea/isa/recordisplay.cfm?deid=347534> (Accessed 20 October 2020),
1129 2019.

1130 Schroder, J. C., Campuzano-Jost, P., Day, D. A., Shah, V., Larson, K., Sommers, J. M., Sullivan,
1131 A. P., Campos, T., Reeves, J. M., Hills, A., Hornbrook, R. S., Blake, N. J., Scheuer, E., Guo, H.,
1132 Fibiger, D. L., McDuffie, E. E., Hayes, P. L., Weber, R. J., Dibb, J. E., Apel, E. C., Jaeglé, L.,
1133 Brown, S. S., Thornton, J. A. and Jimenez, J. L.: Sources and Secondary Production of Organic
1134 Aerosols in the Northeastern US during WINTER, *J. Geophys. Res. D: Atmos.*,
1135 doi:10.1029/2018JD028475, 2018.

1136 Seinfeld, J. H. and Pandis, S. N.: *Atmospheric Chemistry and Physics: From Air Pollution to*
1137 *Climate Change, Second.*, John Wiley & Sons, Inc., Hoboken, NJ USA., 2006.

1138 Seltzer, K. M., Pennington, E., Rao, V., Murphy, B. N., Strum, M., Isaacs, K. K. and Pye, H. O.
1139 T.: Reactive organic carbon emissions from volatile chemical products, *Atmos. Chem. Phys.*, 21,
1140 5079–5100, 2021.

1141 Shaddick, G., Thomas, M. L., Amini, H., Broday, D., Cohen, A., Frostad, J., Green, A., Gumy,
1142 S., Liu, Y., Martin, R. V., Pruss-Ustun, A., Simpson, D., van Donkelaar, A. and Brauer, M.: Data
1143 Integration for the Assessment of Population Exposure to Ambient Air Pollution for Global
1144 Burden of Disease Assessment, *Environ. Sci. Technol.*, 52(16), 9069–9078, 2018.

1145 Shah, V., Jaeglé, L., Thornton, J. A., Lopez-Hilfiker, F. D., Lee, B. H., Schroder, J. C.,
1146 Campuzano-Jost, P., Jimenez, J. L., Guo, H., Sullivan, A. P., Weber, R. J., Green, J. R., Fiddler,
1147 M. N., Bililign, S., Campos, T. L., Stell, M., Weinheimer, A. J., Montzka, D. D. and Brown, S.
1148 S.: Chemical feedbacks weaken the wintertime response of particulate sulfate and nitrate to
1149 emissions reductions over the eastern United States, *Proc. Natl. Acad. Sci. U. S. A.*, 115(32),
1150 8110–8115, 2018.

1151 Shah, V., Jaeglé, L., Jimenez, J. L., Schroder, J. C., Campuzano-Jost, P., Campos, T. L., Reeves,
1152 J. M., Stell, M., Brown, S. S., Lee, B. H., Lopez-Hilfiker, F. D. and Thornton, J. A.: Widespread
1153 Pollution from Secondary Sources of Organic Aerosols during Winter in the Northeastern United
1154 States, *Geophys. Res. Lett.*, doi:10.1029/2018GL081530, 2019.

1155 Shrivastava, M., Cappa, C. D., Fan, J., Goldstein, A. H., Guenther, A. B., Jimenez, J. L., Kuang,
1156 C., Laskin, A., Martin, S. T., Ng, N. L., Petaja, T., Pierce, J. R., Rasch, P. J., Roldin, P., Seinfeld,
1157 J. H., Shilling, J., Smith, J. N., Thornton, J. A., Volkamer, R., Wang, J., Worsnop, D. R., Zaveri,
1158 R. A., Zelenyuk, A. and Zhang, Q.: Recent advances in understanding secondary organic aerosol:

- 1159 Implications for global climate forcing, *Rev. Geophys.*, 55(2), 509–559, 2017.
- 1160 Silva, R. A., Adelman, Z., Fry, M. M. and West, J. J.: The Impact of Individual Anthropogenic
1161 Emissions Sectors on the Global Burden of Human Mortality due to Ambient Air Pollution,
1162 *Environ. Health Perspect.*, 124(11), 1776–1784, 2016.
- 1163 Singh, A., Satish, R. V. and Rastogi, N.: Characteristics and sources of fine organic aerosol over
1164 a big semi-arid urban city of western India using HR-ToF-AMS, *Atmos. Environ.*, 208, 103–112,
1165 2019.
- 1166 Stavroulas, I., Bougiatioti, A., Grivas, G., Paraskevopoulou, D., Tsagkaraki, M., Zarnpas, P.,
1167 Liakakou, E., Gerasopoulos, E. and Mihalopoulos, N.: Sources and processes that control the
1168 submicron organic aerosol composition in an urban Mediterranean environment (Athens): a high
1169 temporal-resolution chemical composition measurement study, *Atmos. Chem. Phys.*, 19(2),
1170 901–919, 2019.
- 1171 Stewart, G. J., Nelson, B. S., Acton, W. J. F., Vaughan, A. R., Farren, N. J., Hopkins, J. R., Ward,
1172 M. W., Swift, S. J., Arya, R., Mondal, A., Jangirh, R., Ahlawat, S., Yadav, L., Sharma, S. K.,
1173 Yunus, S. S. M., Hewitt, C. N., Nemitz, E., Mullinger, N., Gadi, R., Sahu, L. K., Tripathi, N.,
1174 Rickard, A. R., Lee, J. D., Mandal, T. K. and Hamilton, J. F.: Emissions of intermediate-volatility
1175 and semi-volatile organic compounds from domestic fuels used in Delhi, India, *Atmos. Chem.*
1176 *Phys. Discuss.*, doi:10.5194/acp-2020-860, 2020.
- 1177 Toon, O. B., Maring, H., Dibb, J., Ferrare, R., Jacob, D. J., Jensen, E. J., Luo, Z. J., Mace, G. G.,
1178 Pan, L. L., Pfister, L., Rosenlof, K. H., Redemann, J., Reid, J. S., Singh, H. B., Thompson, A.
1179 M., Yokelson, R., Minnis, P., Chen, G., Jucks, K. W. and Pszenny, A.: Planning, implementation,
1180 and scientific goals of the Studies of Emissions and Atmospheric Composition, Clouds and
1181 Climate Coupling by Regional Surveys (SEAC⁴RS) field mission, *J. Geophys. Res. D: Atmos.*,
1182 121(9), 4967–5009, 2016.
- 1183 Tsimpidi, A. P., Karydis, V. A., Zavala, M., Lei, W., Molina, L., Ulbrich, I. M., Jimenez, J. L. and
1184 Pandis, S. N.: Evaluation of the volatility basis-set approach for the simulation of organic aerosol
1185 formation in the Mexico City metropolitan area, *Atmos. Chem. Phys.*, 10(2), 525–546, 2010.
- 1186 Volkamer, R., Jimenez, J. L., San Martini, F., Dzepina, K., Zhang, Q., Salcedo, D., Molina, L. T.,
1187 Worsnop, D. R. and Molina, M. J.: Secondary organic aerosol formation from anthropogenic air
1188 pollution: Rapid and higher than expected, *Geophys. Res. Lett.*, 33(17), L17811, 2006.
- 1189 Wang, L., Slowik, J. G., Tripathi, N., Bhattu, D., Rai, P., Kumar, V., Vats, P., Satish, R.,
1190 Baltensperger, U., Ganguly, D., Rastogi, N., Sahu, L. K., Tripathi, S. N. and Prévôt, A. S. H.:
1191 Source characterization of volatile organic compounds measured by proton-transfer-reaction
1192 time-of-flight mass spectrometers in Delhi, India, *Atmos. Chem. Phys.*, 20(16), 9753–9770,
1193 2020.
- 1194 Warneke, C., de Gouw, J. A., Holloway, J. S., Peischl, J., Ryerson, T. B., Atlas, E., Blake, D.,
1195 Trainer, M. and Parrish, D. D.: Multiyear trends in volatile organic compounds in Los Angeles,

1196 California: Five decades of decreasing emissions, *J. Geophys. Res. D: Atmos.*, 117(D21),
1197 D00V17, 2012.

1198 Wood, E. C., Canagaratna, M. R., Herndon, S. C., Onasch, T. B., Kolb, C. E., Worsnop, D. R.,
1199 Kroll, J. H., Knighton, W. B., Seila, R., Zavala, M., Molina, L. T., Decarlo, P. F., Jimenez, J. L.,
1200 Weinheimer, A. J., Knapp, D. J., Jobson, B. T., Stutz, J., Kuster, W. C. and Williams, E. J.:
1201 Investigation of the correlation between odd oxygen and secondary organic aerosol in Mexico
1202 City and Houston, *Atmos. Chem. Phys.*, 10(18), 8947–8968, 2010.

1203 Woody, M. C., Baker, K. R., Hayes, P. L., Jimenez, J. L., Koo, B. and Pye, H. O. T.:
1204 Understanding sources of organic aerosol during CalNex-2010 using the CMAQ-VBS, *Atmos.*
1205 *Chem. Phys.*, 16(6), 4081–4100, 2016.

1206 Worton, D. R., Isaacman, G., Gentner, D. R., Dallmann, T. R., Chan, A. W. H., Ruehl, C.,
1207 Kirchstetter, T. W., Wilson, K. R., Harley, R. A. and Goldstein, A. H.: Lubricating Oil Dominates
1208 Primary Organic Aerosol Emissions from Motor Vehicles, *Environ. Sci. Technol.*, 48(7),
1209 3698–3706, 2014.

1210 Ye, P., Ding, X., Hakala, J., Hofbauer, V., Robinson, E. S. and Donahue, N. M.: Vapor wall loss
1211 of semi-volatile organic compounds in a Teflon chamber, *Aerosol Sci. Technol.*, 50(8), 822–834,
1212 2016.

1213 Zhang, Q., Jimenez, J. L., Canagaratna, M. R., Allan, J. D., Coe, H., Ulbrich, I., Alfarra, M. R.,
1214 Takami, A., Middlebrook, A. M., Sun, Y. L., Dzepina, K., Dunlea, E., Docherty, K., DeCarlo, P.
1215 F., Salcedo, D., Onasch, T., Jayne, J. T., Miyoshi, T., Shimono, A., Hatakeyama, S., Takegawa,
1216 N., Kondo, Y., Schneider, J., Drewnick, F., Borrmann, S., Weimer, S., Demerjian, K., Williams,
1217 P., Bower, K., Bahreini, R., Cottrell, L., Griffin, R. J., Rautiainen, J., Sun, J. Y., Zhang, Y. M. and
1218 Worsnop, D. R.: Ubiquity and dominance of oxygenated species in organic aerosols in
1219 anthropogenically-influenced Northern Hemisphere midlatitudes, *Geophys. Res. Lett.*, 34(13),
1220 L13801, 2007.

1221 Zhang, Q. J., Beekmann, M., Freney, E., Sellegri, K., Pichon, J. M., Schwarzenboeck, A.,
1222 Colomb, A., Bourrienne, T., Michoud, V. and Borbon, A.: Formation of secondary organic
1223 aerosol in the Paris pollution plume and its impact on surrounding regions, *Atmos. Chem. Phys.*,
1224 15(24), 13973–13992, 2015.

1225 Zhao, B., Wang, S., Donahue, N. M., Jathar, S. H., Huang, X., Wu, W., Hao, J. and Robinson, A.
1226 L.: Quantifying the effect of organic aerosol aging and intermediate-volatility emissions on
1227 regional-scale aerosol pollution in China, *Sci. Rep.*, 6, 28815, 2016a.

1228 Zhao, Y., Hennigan, C. J., May, A. A., Daniel, S., Gouw, J. A. D., Gilman, J. B., Kuster, W. C.
1229 and Robinson, A. L.: Intermediate-Volatility Organic Compounds: A Large Source of Secondary
1230 Organic Aerosol, *Environ. Sci. Technol.*, 48(23), 13743–13750, 2014.

1231 Zhao, Y., Nguyen, N. T., Presto, A. A., Hennigan, C. J., May, A. A. and Robinson, A. L.:
1232 Intermediate Volatility Organic Compound Emissions from On-Road Gasoline Vehicles and

1233 Small Off-Road Gasoline Engines, *Environ. Sci. Technol.*, 50(8), 4554–4563, 2016b.

1234 Zhao, Y., Saleh, R., Saliba, G., Presto, A. A., Gordon, T. D., Drozd, G. T., Goldstein, A. H.,
1235 Donahue, N. M. and Robinson, A. L.: Reducing secondary organic aerosol formation from
1236 gasoline vehicle exhaust, *Proc. Natl. Acad. Sci. U. S. A.*, 114(27), 6984–6989, 2017.

1237